

Neutrino energy loss rate in a stellar plasma

S. Esposito, G. Mangano, G. Miele, I. Picardi, and O. Pisanti

Dipartimento di Scienze Fisiche, Università di Napoli “Federico II”

and

Istituto Nazionale di Fisica Nucleare, Sezione di Napoli

Complesso Universitario di Monte S. Angelo, Via Cinthia, I-80126 Napoli, Italy

*E-mail: sesposito@na.infn.it, mangano@na.infn.it, miele@na.infn.it, picardi@na.infn.it,
pisanti@na.infn.it*

Abstract

We review the purely leptonic neutrino emission processes, contributing to the energy loss rate of the stellar plasma. We perform a complete analysis up to the first order in the electromagnetic coupling constant. In particular the radiative electromagnetic corrections, at order α , to the process $e^+e^- \rightarrow \nu\bar{\nu}$ at finite density and temperature have been computed. This process gives one of the main contributions to the cooling of stellar interior in the late stages of star evolution. As a result of the analysis we find that the corrections affect the energy loss rate, computed at tree level, by a factor $(-4 \div 1)\%$ in the temperature and density region where the pair annihilation is the most efficient cooling mechanism.

PACS number(s): 13.40.Ks, 95.30.Cq, 11.10.Wx

1 Introduction

One of the crucial parameters which strongly affect the stellar evolution is the cooling rate. Stars during their life can emit energy in the form of electromagnetic or gravitational waves, and/or as a flux of neutrinos. However, in late stages a star mainly loses energy through neutrinos, and this is pretty independent of the mass of the star. In fact, white dwarfs and Supernovae, which are the end points for stars with very different masses, have both cooling rates largely dominated by neutrino production. An accurate determination of neutrino emission rates is therefore mandatory in order to perform a careful study of the final branches of star evolutionary tracks. In particular, a change in the cooling rates at the very last stages of massive star evolution could sensibly affect the evolutionary time scale and the iron core configuration at the onset of the Supernova explosion, whose triggering mechanism is still lacking a full theoretical understanding [1].

The energy loss rate due to neutrino emission (hereafter denoted by Q) receives contribution from both weak nuclear reactions and purely leptonic processes. However for the rather large values of density and temperature which characterize the final stages of stellar evolution, the latter are largely dominant. The leading leptonic processes are the following:

- i) pair annihilation $e^+ + e^- \rightarrow \nu + \bar{\nu}$
- ii) ν -photoproduction $\gamma + e^\pm \rightarrow e^\pm + \nu + \bar{\nu}$
- iii) plasmon decay $\gamma^* \rightarrow \nu + \bar{\nu}$
- iv) bremsstrahlung on nuclei $e^\pm + Z \rightarrow e^\pm + Z + \nu + \bar{\nu}$

Each process above results to be the dominant contribution to Q in different regions of the core density–temperature plane. For very large core temperatures, $T \gtrsim 10^9 \text{ }^\circ\text{K}$, and relatively low density, $\rho \lesssim 10^5 \text{ g cm}^{-3}$, the pair annihilation is the most efficient cooling process. For the same values of densities but lower temperatures, $10^8 \text{ }^\circ\text{K} \lesssim T \lesssim 10^9 \text{ }^\circ\text{K}$, the ν -photoproduction gives the leading contribution. These density-temperature ranges are the typical ones for very massive stars in their late evolution. Finally, plasmon decay and bremsstrahlung on nuclei are mostly important for large ($\rho \gtrsim 10^6 \text{ g cm}^{-3}$) and

extremely large ($\rho \gtrsim 10^9 \text{ g cm}^{-3}$) core densities, respectively, and temperatures of the order of $10^8 \text{ }^\circ\text{K} \lesssim T \lesssim 10^{10} \text{ }^\circ\text{K}$. Such conditions are typically realized in white dwarfs.

Starting from the first calculations of Ref.s [2, 3], a systematic study of the energy loss rates for processes i)–iv) has been performed in a long series of papers [2]–[22]. In all these analyses the pair production rate i) has been evaluated at order G_F^2 , i.e. at the zero–order in the electromagnetic coupling constant α expansion, whereas the remaining processes ii)–iv) are at least of order αG_F^2 . Thus to correctly compare the energy loss rates for all processes i)–iv) it is worth computing QED radiative corrections to pair annihilation rate i), which may lead to a sensible change in the cooling rate Q . This is the aim of our analysis, whose results have been briefly reported in Ref. [23]. In this paper we give all the details of the calculations.

The paper is organized as follows. Section 2 is devoted to a brief summary of Born amplitude calculation for pair process, while in Section 3 we report the details of order α QED corrections. Neutrino photoproduction and plasmon decay are discussed in Section 4 and 5, respectively. Our results are summarized in Section 6.

2 Born amplitude for pair annihilation process

Let us consider the annihilation process $e^-(p_1) + e^+(p_2) \rightarrow \nu_\alpha(q_1) + \bar{\nu}_\alpha(q_2)$, where $\alpha = e, \mu, \tau$, and the 4–momenta are defined as $p_{1,2} \equiv (E_{1,2}, \mathbf{p}_{1,2})$ and $q_{1,2} \equiv (\omega_{1,2}, \mathbf{q}_{1,2})$. The energy loss rate induced by this process is obtained by integrating the squared modulus of the invariant amplitude $M_{e^+e^- \rightarrow \nu_\alpha \bar{\nu}_\alpha}$ over the phase-space of the involved particles, and summing over the flavour of final neutrinos,

$$Q_{e^+e^-} = \frac{1}{(2\pi)^6} \int \frac{d^3\mathbf{p}_1}{2E_1} \int \frac{d^3\mathbf{p}_2}{2E_2} (E_1 + E_2) F_-(E_1) F_+(E_2) \\ \times \left\{ \frac{1}{(2\pi)^2} \int \frac{d^3\mathbf{q}_1}{2\omega_1} \int \frac{d^3\mathbf{q}_2}{2\omega_2} \delta^{(4)}(p_1 + p_2 - q_1 - q_2) \sum_{spin,\alpha} |M_{e^+e^- \rightarrow \nu_\alpha \bar{\nu}_\alpha}|^2 \right\} . \quad (2.1)$$

The quantities $F_\pm(E) = [\exp\{\frac{E}{T} \pm \xi_e\} + 1]^{-1}$ are the Fermi-Dirac distribution functions for e^\pm with temperature T and degeneracy parameter ξ_e , and in $\sum_{spin,\alpha}$ a sum over all particle polarizations and final flavours is performed. Notice that, as long as neutrino mean free path is large enough that they can leave the star without any further inter-

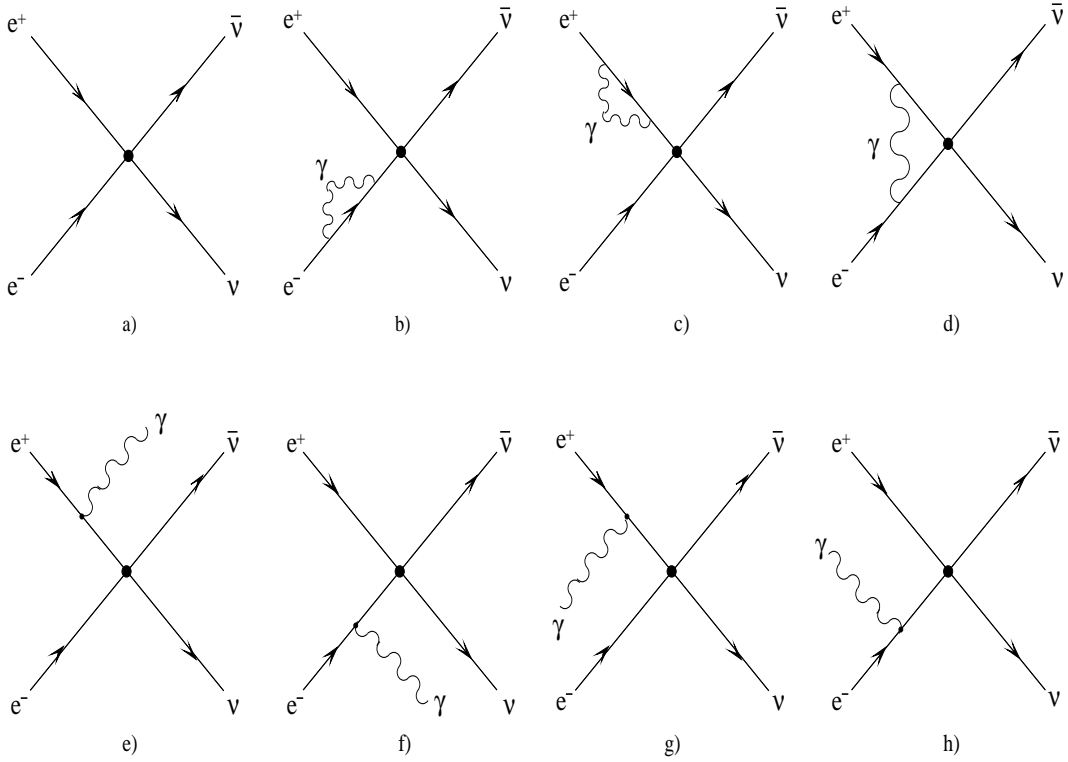


Figure 1: Feynman diagrams for the pair annihilation process up to order αG_F^2 .

action, there is no relevant neutrino component in the stellar plasma. Thus no neutrino distribution function is present in the expression for the energy loss rate.

In this Section we evaluate $Q_{e^+e^-}$ in the Born approximation (hereafter denoted with $Q_{e^+e^-}^B$), i.e. in the limit of a four-fermion electroweak interaction and no electromagnetic radiative correction (see Figure 1a). Let us consider first the pair annihilation in electron neutrinos. At first order in perturbation theory, the diagram in Figure 1a contributes to the invariant amplitude $M_{e^+e^- \rightarrow \nu_e \bar{\nu}_e}$ with two terms coming from W^\pm and Z^0 boson exchange, respectively. By using the low energy expression for the vector boson propagators, one has¹

$$M_{e^+e^- \rightarrow \nu_e \bar{\nu}_e}^W = -\frac{g^2}{8m_W^2} [\bar{u}(q_1)\gamma_\mu(1-\gamma_5)u(p_1)] [\bar{v}(p_2)\gamma^\mu(1-\gamma_5)v(q_2)] , \quad (2.2)$$

and

$$M_{e^+e^- \rightarrow \nu_e \bar{\nu}_e}^Z = -\frac{g^2}{8\cos^2\theta_W m_Z^2} [\bar{v}(p_2)\gamma_\mu(C_V - C_A\gamma_5)u(p_1)] [\bar{u}(q_1)\gamma^\mu(1-\gamma_5)v(q_2)] , \quad (2.3)$$

¹We use natural units, $\hbar = c = k = 1$.

where $C_V = 2 \sin^2 \theta_W - 1/2$, $C_A = -1/2$ and $\alpha = e, \mu, \tau$. By using a Fierz transformation on Eq.(2.2) and summing it to (2.3) one gets the total amplitude in Born approximation,

$$M_{e^+e^- \rightarrow \nu_e \bar{\nu}_e}^B = -\frac{G_F}{\sqrt{2}} [\bar{u}(q_1)\gamma_\mu(1 - \gamma_5)v(q_2)] [\bar{v}(p_2)\gamma^\mu(C_V' - C_A'\gamma_5)u(p_1)] , \quad (2.4)$$

with

$$C_V' = 1 + C_V = \frac{1}{2} + 2 \sin^2 \theta_W , \quad (2.5)$$

$$C_A' = 1 + C_A = \frac{1}{2} . \quad (2.6)$$

The squared modulus of the amplitude (2.4), summed on the polarizations of the incoming and outgoing particles, can be expressed as the product of the two tensors, $T_{\mu\nu}^{(e)}$ and $T_{\mu\nu}^{(\nu)}$,

$$\sum_{spin} |M_{e^+e^- \rightarrow \nu_e \bar{\nu}_e}^B|^2 = \frac{G_F^2}{2} T_{\mu\nu}^{(e)} T^{(\nu)\mu\nu} . \quad (2.7)$$

The tensors $T_{\mu\nu}^{(e)}$ and $T_{\mu\nu}^{(\nu)}$ in Eq.(2.7) can be both decomposed in a symmetric (S) and antisymmetric (A) part in the indices $\mu\nu$, namely

$$S_{\mu\nu}^{(e,\nu)} \equiv \frac{T_{\mu\nu}^{(e,\nu)} + T_{\nu\mu}^{(e,\nu)}}{2} , \quad (2.8)$$

$$A_{\mu\nu}^{(e,\nu)} \equiv \frac{T_{\mu\nu}^{(e,\nu)} - T_{\nu\mu}^{(e,\nu)}}{2} . \quad (2.9)$$

In their product only the SS and AA combinations survive, but the latter disappears after performing the integration over neutrino phase spaces. This integration can be performed by using the Lenard formula, namely

$$\int \frac{d^3 \mathbf{q}_1}{2\omega_1} \int \frac{d^3 \mathbf{q}_2}{2\omega_2} \delta^{(4)}(p - q_1 - q_2) q_1^\alpha q_2^\beta = \frac{\pi}{24} (2p^\alpha p^\beta + g^{\alpha\beta} p^2) \Theta(p^0) \Theta(p^2) , \quad (2.10)$$

where p^μ denotes a generic 4-momentum. By means of Eq.(2.10), the quantity in curly brackets of Eq.(2.1), but only for electron neutrinos, takes the form

$$\begin{aligned} & \frac{1}{(2\pi)^2} \int \frac{d^3 \mathbf{q}_1}{2\omega_1} \int \frac{d^3 \mathbf{q}_2}{2\omega_2} \delta^{(4)}(p_1 + p_2 - q_1 - q_2) \sum_{spin} |M_{e^+e^- \rightarrow \nu_e \bar{\nu}_e}^B|^2 \\ &= \frac{8G_F^2}{3\pi} (m_e^2 + p_1 \cdot p_2) \left[(C_V'^2 + C_A'^2) p_1 \cdot p_2 + (2C_V'^2 - C_A'^2) m_e^2 \right] . \end{aligned} \quad (2.11)$$

For ν_μ or ν_τ production, the W^\pm exchange term is instead absent and thus only the neutral current contributes. In this case, by using the previous arguments the same expression

(2.11) is obtained but with the substitution $C_V', C_A' \rightarrow C_V, C_A$. By virtue of the above results, the total $Q_{e^+e^-}^B$, obtained by summing on neutrino flavour, reads

$$Q_{e^+e^-}^B = \frac{G_F^2 m_e^4}{18\pi^5} \int_0^\infty \frac{|\mathbf{p}_1|^2 d|\mathbf{p}_1|}{E_1} \int_0^\infty \frac{|\mathbf{p}_2|^2 d|\mathbf{p}_2|}{E_2} (E_1 + E_2) F_-(E_1) F_+(E_2) \\ \times \left[C_V'^2 \left(\frac{4 E_1^2 E_2^2}{m_e^4} + \frac{9 E_1 E_2}{m_e^2} - \frac{E_1^2 + E_2^2}{m_e^2} + 9 \right) + C_A'^2 \left(\frac{4 E_1^2 E_2^2}{m_e^4} - \frac{E_1^2 + E_2^2}{m_e^2} \right) \right], \quad (2.12)$$

where we have denoted with $C_{V,A}^{\prime 2} \equiv (1 + C_{V,A})^2 + 2C_{V,A}^2$ and we have performed the angular integrations. Note that $Q_{e^+e^-}^B$ depends on the temperature T and the electron degeneracy parameter ξ_e only.

It is customary to recast the dependence of the energy loss rate on ξ_e (or the electron chemical potential) in terms of the matter density, ρ , the temperature, T , and the electron molecular weight, μ_e ,

$$\frac{1}{\mu_e} \equiv \sum_i X_i \frac{Z_i}{A_i}, \quad (2.13)$$

where in the above expression the sum is performed over all nuclides, Z_i and A_i stand for the atomic and the weight number of the i -nuclide, respectively, and X_i is its mass fraction. To this aim, by requiring the electrical neutrality of the plasma, we have

$$n_{e^-} - n_{e^+} = N_A \frac{\rho}{\mu_e}, \quad (2.14)$$

where n_{e^\pm} are the e^\pm number densities and N_A is the Avogadro number. The degeneracy parameter ξ_e can be then obtained by inverting Eq.(2.14), namely

$$\frac{\rho}{\mu_e} = \frac{1}{\pi^2 N_A} \int_{m_e}^\infty E \sqrt{E^2 - m_e^2} dE \left(\frac{1}{\exp\left\{\frac{E}{T} - \xi_e\right\} + 1} - \frac{1}{\exp\left\{\frac{E}{T} + \xi_e\right\} + 1} \right). \quad (2.15)$$

Once performed numerically the integration over electron/positron momenta in Eq.(2.12), the energy loss rate due to pair annihilation in the Born approximation can be expressed as a function of T and ρ/μ_e only. The results are shown in Figure 2, where $Q_{e^+e^-}^B$ is plotted as a function of ρ/μ_e , for the following values of temperature $T = 10^8, 10^{8.5}, 10^9, 10^{10}$ °K.

3 Radiative corrections to pair annihilation

A consistent computation of the αG_F^2 corrections to the energy loss rate induced by pair annihilation is obtained by considering in addition to the tree level graph of Figure 1a,

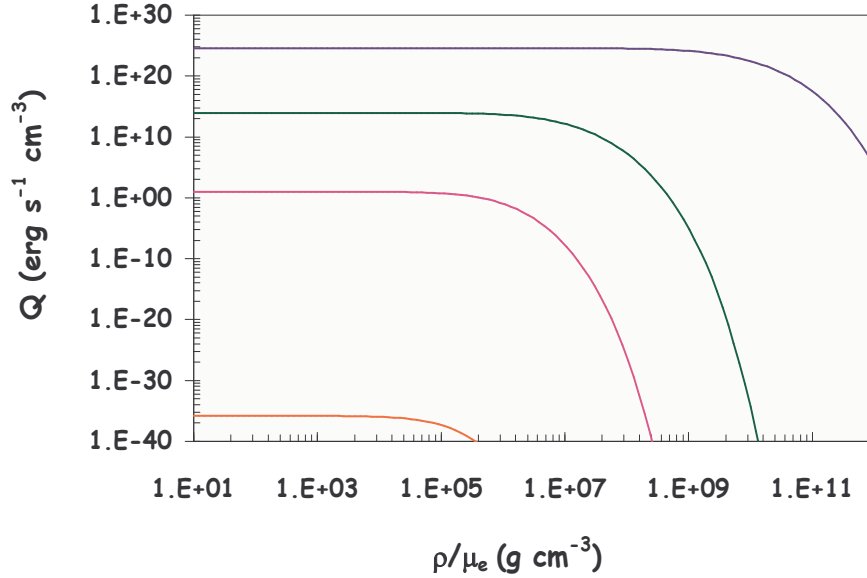


Figure 2: The energy loss rate due to pair annihilation process in the Born approximation, $Q_{e^+e^-}^B$, is here plotted for $T = 10^8, 10^{8.5}, 10^9, 10^{10}$ °K (from bottom to top).

the *radiative* diagrams of Figures 1b-1h. The corrections of order αG_F^2 are then obtained *via* their interference.

It is worth while observing that since the typical energy carried by the outgoing neutrino pair is at most of the order of 1 MeV, one can safely neglect the electroweak radiative corrections to the four-fermion effective interaction (involving additional weak boson propagators), and only consider the gauge-invariant set of purely QED contributions.

When the processes we consider take place in stellar interiors, we must take into account the influence of the electromagnetic plasma (namely, e^\pm, γ) when computing radiative corrections. To this end we have performed calculations by using the Real Time Formalism for finite temperature quantum field theory. In this framework the thermal propagators for electrons and photons read as follow

$$i S(p) = (\not{p} + m) \left[\frac{i}{p^2 - m_e^2 + i\epsilon} - \Gamma_F(p) \right] , \quad (3.16)$$

$$i D_{\alpha\beta}(k) = -g_{\alpha\beta} \left[\frac{i}{k^2 + i\epsilon} + \Gamma_B(k) \right] , \quad (3.17)$$

with

$$\Gamma_F(p) = 2\pi \delta(p^2 - m_e^2) [F_-(|p_0|)\Theta(p_0) + F_+(|p_0|)\Theta(-p_0)] , \quad (3.18)$$

$$\Gamma_B(k) = 2\pi \delta(k^2) B(|k_0|) , \quad (3.19)$$

where $\Theta(x)$ is the step function and $B(x)$ is the Bose-Einstein distribution function. The first terms in Eqs.(3.16) and (3.17) are the usual $T = 0$ Feynman propagators, while those depending on the temperature (and density) through the distribution functions describe the interactions with real particles of the thermal bath.

According to the different diagrams contributing to radiative corrections, it is customary to classify these corrections as follows:

- electron mass and wavefunction renormalization (Figures 1b–1c);
- electromagnetic vertex correction (Figure 1d);
- γ emission/absorption (Figures 1e–1h).

3.1 Zero–temperature radiative correction

By using in the evaluation of radiative corrections of Figures 1b-1d the first term only in the propagators of Eqs.(3.16),(3.17), one obtains the off-shell contribution to the radiative amplitude, and the corresponding result is known as zero–temperature or vacuum correction.

This issue has been addressed in Ref. [24] for the process $e^- + \nu \rightarrow e^- + \nu$, but we can easily obtain the desired corrections for pair annihilation by using crossing symmetry. The vacuum correction to be inserted into Eq.(2.1) is then

$$\sum_{spin,\alpha} |\Delta M_{e^+e^- \rightarrow \nu\alpha\bar{\nu}\alpha}^{T=0}|^2 = \frac{128}{\pi} \alpha G_F^2 m_e^2 \omega_2^2 \delta(E_2, \omega_2) , \quad (3.20)$$

where

$$\begin{aligned} \delta(E_2, \omega_2) &= g_L^2 \left\{ V_1(E_2) + V_2(E_2) \left[z - 1 + \frac{m_e z}{2\omega_2} \right] \right\} \\ &+ g_R^2 \left\{ V_1(E_2) (1 - z)^2 + V_2(E_2) \left[z - 1 + \frac{m_e z}{2\omega_2} \right] \right\} \\ &+ g_{LR} \left\{ [V_1(E_2) - V_2(E_2)] \left(\frac{m_e z}{\omega_2} \right) - 2 V_2(E_2) [z - 1 - z^2] \right\} , \quad (3.21) \end{aligned}$$

$$V_1(E_2) = \text{Re} \left\{ \left(2 \log \frac{m_e}{\lambda} \right) \left[1 - \frac{E_2}{2|\mathbf{p}_2|} \log \left(\frac{E_2 + |\mathbf{p}_2|}{E_2 - |\mathbf{p}_2|} \right) \right] - 2 - \frac{E_2}{|\mathbf{p}_2|} \left[\text{Li}_2 \left(\frac{|\mathbf{p}_2| - E_2 - m_e}{2|\mathbf{p}_2|} \right) \right] \right\}$$

$$- \text{Li}_2 \left(\frac{|\mathbf{p}_2| + E_2 + m_e}{2|\mathbf{p}_2|} \right) \Big] - \frac{1}{4|\mathbf{p}_2|} \left[-3E_2 + m_e + E_2 \log \left(\frac{2m_e - 2E_2}{m_e} \right) \right] \log \left(\frac{E_2 + |\mathbf{p}_2|}{E_2 - |\mathbf{p}_2|} \right) \Big\} , \quad (3.22)$$

$$V_2(E_2) = -\frac{m_e}{4|\mathbf{p}_2|} \log \left(\frac{E_2 + |\mathbf{p}_2|}{E_2 - |\mathbf{p}_2|} \right) , \quad (3.23)$$

with

$$g_L^2 = 3 \sin^4 \theta_w - \sin^2 \theta_w + \frac{3}{4} , \quad (3.24)$$

$$g_R^2 = 3 \sin^4 \theta_w , \quad (3.25)$$

$$g_{LR} = \sin^2 \theta_w \left(3 \sin^2 \theta_w - \frac{1}{2} \right) , \quad (3.26)$$

$z = (E_2 + m_e)/\omega_2$ and λ is a small photon mass introduced to regularize the infrared divergences. Remind that the dilogarithm function $\text{Li}_2(x)$ is defined by

$$\text{Li}_2(x) \equiv - \int_0^x dt \frac{\log(1-t)}{t} . \quad (3.27)$$

The expression (3.20) depends on the infrared regulator λ and diverges for $\lambda \rightarrow 0$. This is quite obvious since as it is well known, when computing QED radiative corrections, in addition to the pair annihilation process one must consider also the bremsstrahlung radiation accompanying the process (Figures 1e-1h). In fact, only the combination of virtual and real photon corrections is free from infrared divergencies.

The bremsstrahlung process will be considered in detail in Section 3.2.3 but here we anticipate the strategy for a careful and reliable numerical computation of the integrals in Eq.(3.33). In fact, numerical cancellation of divergencies is very hard to handle and we prefer to divide the bremsstrahlung contribution into a “soft” part (according to the photon energy being lower than some fixed threshold ϵ) which will cancel the infrared divergencies of the pair process, and a “hard” one which, in our case, will depend on the thermal photon distribution function. The last one will be considered in Section 3.2.3 while we now report the Soft-Bremsstrahlung (S.B.) squared modulus. Again we use the result of Ref. [24] with a suitable crossing transformation and thus we get

$$\sum_{spin,\alpha} |\Delta M_{e^+e^- \rightarrow \nu_\alpha \bar{\nu}_\alpha}^{S.B.}|^2 = \frac{128}{\pi} \alpha G_F^2 m_e^2 \omega_2^2 I_\gamma(E_2, \epsilon) \left[g_L^2 + g_R^2 (1-z)^2 + g_{LR} \left(\frac{m_e z}{\omega_2} \right) \right] , \quad (3.28)$$

where

$$I_\gamma(E_2, \epsilon) = \text{Re} \left\{ \left(2 \log \frac{\lambda}{\epsilon} \right) \left[1 - \frac{E_2}{2|\mathbf{p}_2|} \log \left(\frac{E_2 + |\mathbf{p}_2|}{E_2 - |\mathbf{p}_2|} \right) \right] + \frac{E_2}{2|\mathbf{p}_2|} \left[L \left(\frac{E_2 + |\mathbf{p}_2|}{E_2 - |\mathbf{p}_2|} \right) - L \left(\frac{E_2 - |\mathbf{p}_2|}{E_2 + |\mathbf{p}_2|} \right) + \log \left(\frac{E_2 + |\mathbf{p}_2|}{E_2 - |\mathbf{p}_2|} \right) \left(1 - 2 \log \left(\frac{|\mathbf{p}_2|}{m_e} \right) \right) \right] + 1 - 2 \log 2 \right\} , \quad (3.29)$$

and

$$L(x) \equiv \int_0^x dt \frac{\log |1-t|}{t} . \quad (3.30)$$

Remarkably, by summing the expressions (3.20) and (3.28), since the term $[V_1(E_2) + I_\gamma(E_2, \epsilon)]$ does not depend on the infrared regulator λ , the total squared amplitude is now infrared divergence free. Then, the term in curly brackets in Eq.(2.1), once integrating over all variables but one by using the δ -function, becomes:

$$\begin{aligned} \Phi &\equiv \frac{1}{(2\pi)^2} \int \frac{d^3 \mathbf{q}_1}{2\omega_1} \int \frac{d^3 \mathbf{q}_2}{2\omega_2} \delta^{(4)}(p_1 + p_2 - q_1 - q_2) \\ &\times \sum_{spin, \alpha} \left(|\Delta M_{e^+e^- \rightarrow \nu_\alpha \bar{\nu}_\alpha}^{T=0}|^2 + |\Delta M_{e^+e^- \rightarrow \nu_\alpha \bar{\nu}_\alpha}^{S.B.}|^2 \right) \\ &= \frac{16 \alpha G_F^2 m_e^2}{\pi^2} \int_{\omega_m}^{\omega_M} d\omega'_2 \frac{\omega_2'^2}{|\mathbf{p}'_2|} \\ &\times \left\{ \delta(E'_2, \omega'_2) + I_\gamma(E'_2, \epsilon) \left[g_L^2 + g_R^2 (1 - z')^2 + g_{LR} \left(\frac{m_e z'}{\omega_2} \right) \right] \right\} , \quad (3.31) \end{aligned}$$

where we denote with a prime the quantities in the electron rest frame, and the integration limits are

$$\omega_m = m_e \frac{E'_2 + m_e}{E'_2 + |\mathbf{p}'_2| + m_e} , \quad \omega_M = m_e \frac{E'_2 + m_e}{E'_2 - |\mathbf{p}'_2| + m_e} . \quad (3.32)$$

Using this result, the correction to the energy loss rate at zero-temperature is

$$\Delta Q_{e^+e^-}^{T=0} = \frac{1}{32 \pi^4} \int_0^\infty d|\mathbf{p}_1| d|\mathbf{p}_2| \int_{-1}^1 d(\cos \theta_{12}) |\mathbf{p}_1|^2 |\mathbf{p}_2|^2 \frac{E_1 + E_2}{E_1 E_2} \hat{\Phi} F_-(E_1) F_+(E_2) , \quad (3.33)$$

where θ_{12} is the angle between \mathbf{p}_1 and \mathbf{p}_2 , $\hat{\Phi}$ stands for Φ boosted to the comoving frame and the integrals must be numerically evaluated.

3.2 Thermal radiative corrections

The *true* thermal radiative corrections to the Born estimate of the neutrino pair production process come from considering in the evaluation of radiative diagrams of Figures 1b-1d the terms involving at least one thermal part of the propagators (3.16) and (3.17).

These contributions do not involve ultraviolet divergencies due to the presence of the Fermi and Bose function in the thermal propagators. Nevertheless, the results corresponding to each of these corrections are not free from infrared divergencies and, in general, are gauge-dependent too. The inclusion in our calculations of the photon emission/absorption diagrams in Figures 1e-1h is then required to overcome these difficulties, as we have directly and carefully checked. In the intermediate steps, however, we have to regularize the actual divergences and, to this end, we have explicitly subtracted all divergent terms expanding the squared amplitudes in a Laurent series around the pole singularities. This method follows quite closely what has been already used in Refs. [25], [26].

3.2.1 Mass and wavefunction renormalization at finite temperature

As already stated, at order α , the e^\pm thermal mass shift and thermal wavefunction renormalization corrections come from the interference of the diagrams in Figures 1b-1c with the tree-level one of Figure 1a, having subtracted the zero-temperature contribution.

The thermal mass correction to neutrino energy loss rate may be obtained by replacing e^\pm mass m_e with the renormalized value $m_{e^\pm}^R = m_e + \delta m_\pm$ in the Born expression for the rate and subtracting the zero-temperature limit (2.12). The self-energy for an electron of energy E and momentum \mathbf{p} has been calculated in Ref. [26] and we refer the reader to this paper for details. At order α the thermal mass shift for e^\pm is given by

$$\begin{aligned} \delta m_\pm &= \frac{\alpha\pi}{3m_e} T^2 + \frac{\alpha}{\pi m_e} \int_0^\infty d|\mathbf{k}| \frac{|\mathbf{k}|^2}{E_k} (F_\pm(E_k) + F_\mp(E_k)) \\ &+ \frac{\alpha m_e}{2\pi|\mathbf{p}|} \int_0^\infty d|\mathbf{k}| \frac{|\mathbf{k}|}{E_k} (F_\pm(E_k) \log C_- + F_\mp(E_k) \log C_+) \quad , \end{aligned} \quad (3.34)$$

with

$$C_\pm = \frac{m_e^2 + |\mathbf{p}||\mathbf{k}| \pm E E_k}{m_e^2 - |\mathbf{p}||\mathbf{k}| \pm E E_k} \quad , \quad (3.35)$$

where $E_k = \sqrt{|\mathbf{k}|^2 + m_e^2}$ and $E = \sqrt{|\mathbf{p}|^2 + m_e^2}$. By using the thermal renormalized masses in the expressions for energies appearing in the Born rate in Eq.(2.12), after some algebra we obtain the following thermal mass correction to the neutrino energy loss rate

$$\Delta Q_{e^+e^-}^M = \Delta Q_{e^+e^-}^{M,B} + \Delta Q_{e^+e^-}^{M,F+} + \Delta Q_{e^+e^-}^{M,F-} \quad , \quad (3.36)$$

with

$$\begin{aligned} \Delta Q_{e^+e^-}^{M,B} &= \frac{\alpha G_F^2}{9\pi^6} \int_0^\infty d|\mathbf{p}_1|d|\mathbf{p}_2|d|\mathbf{k}| |\mathbf{p}_1|^2|\mathbf{p}_2|^2|\mathbf{k}| \left(\frac{1}{E_1} + \frac{1}{E_2} \right) \\ &\quad \times F_-(E_1)F_+(E_2)B(|\mathbf{k}|) \left(\frac{f_1}{E_1} + \frac{f_2}{E_2} \right) , \end{aligned} \quad (3.37)$$

$$\begin{aligned} \Delta Q_{e^+e^-}^{M,F_\pm} &= \frac{\alpha G_F^2}{18\pi^6} \int_0^\infty d|\mathbf{p}_1|d|\mathbf{p}_2|d|\mathbf{k}| \frac{|\mathbf{p}_1|^2|\mathbf{p}_2|^2|\mathbf{k}|}{E_k} \left(\frac{1}{E_1} + \frac{1}{E_2} \right) F_-(E_1)F_+(E_2)F_\pm(E_k) \\ &\quad \times \left[|\mathbf{k}| \left(\frac{f_1}{E_1} + \frac{f_2}{E_2} \right) + \frac{m_e^2}{2} \left(\frac{f_1}{E_1|\mathbf{p}_1|} \log C_{\pm 1} + \frac{f_2}{E_2|\mathbf{p}_2|} \log C_{\mp 2} \right) \right] , \end{aligned} \quad (3.38)$$

$$\begin{aligned} f_1 &= \frac{E_2}{m_e} \left[(C_A'^2 + C_V'^2) \left(3 + 6 \frac{E_1 E_2}{m_e^2} \right) - 3(C_A'^2 - 2C_V'^2) \right] - m_e \left(\frac{E_2}{E_1(E_1 + E_2)} \right. \\ &\quad \left. + \frac{1 - F_-(E_1)}{T} \right) \left\{ (C_A'^2 + C_V'^2) \left[3 \frac{E_1 E_2}{m_e^2} \left(1 + \frac{E_1 E_2}{m_e^2} \right) + \frac{|\mathbf{p}_1|^2|\mathbf{p}_2|^2}{m_e^4} \right] \right. \\ &\quad \left. - 3(C_A'^2 - 2C_V'^2) \left(1 + \frac{E_1 E_2}{m_e^2} \right) \right\} , \end{aligned} \quad (3.39)$$

$$\begin{aligned} f_2 &= \frac{E_1}{m_e} \left[(C_A'^2 + C_V'^2) \left(3 + 6 \frac{E_1 E_2}{m_e^2} \right) - 3(C_A'^2 - 2C_V'^2) \right] - m_e \left(\frac{E_1}{E_2(E_1 + E_2)} \right. \\ &\quad \left. + \frac{1 - F_+(E_2)}{T} \right) \left\{ (C_A'^2 + C_V'^2) \left[3 \frac{E_1 E_2}{m_e^2} \left(1 + \frac{E_1 E_2}{m_e^2} \right) + \frac{|\mathbf{p}_1|^2|\mathbf{p}_2|^2}{m_e^4} \right] \right. \\ &\quad \left. - 3(C_A'^2 - 2C_V'^2) \left(1 + \frac{E_1 E_2}{m_e^2} \right) \right\} , \end{aligned} \quad (3.40)$$

where $C_{\pm 1,2}$ are obtained from C_\pm in Eq.(3.35) with the substitution $(E, \mathbf{p}) \rightarrow (E_{1,2}, \mathbf{p}_{1,2})$.

Note that in Eq.(3.36) we have subtracted all divergent terms as described above.

Diagrams in Figures 1b–1c are also responsible for the thermal wavefunction renormalization correction which, in the calculation for the neutrino energy loss rate, can be obtained by using a thermal renormalized projector on positive/negative energy states as described in Refs. [25, 26]. The projector on positive energy states for an electron of 4-momentum $p \equiv (E, \mathbf{p})$ can be cast in the following form

$$\Lambda_R^+ = \frac{\not{p} + m_e^R + \delta_+}{2E} , \quad (3.41)$$

$$\delta_+ = (\not{p} + m_e)\mathcal{A} + \left(\not{\tilde{p}} - \frac{|\mathbf{p}|^2}{m_e} \right) \mathcal{B} , \quad (3.42)$$

with $\tilde{p} = (0, \mathbf{p})$ and where the momentum-dependent functions \mathcal{A} and \mathcal{B} are given by

$$\mathcal{A} = \frac{\alpha}{2\pi E} \int_0^\infty d|\mathbf{k}| |\mathbf{k}| \left[-\frac{2B(|\mathbf{k}|)}{|\mathbf{p}|} \log \left(\frac{E + |\mathbf{p}|}{E - |\mathbf{p}|} \right) + F_-(E_k) \left(\frac{2|\mathbf{k}|}{(E - E_k)^2} + \frac{\log C_-}{|\mathbf{p}|} \right) \right]$$

$$- F_+(E_k) \left(\frac{2|\mathbf{k}|}{(E + E_k)^2} + \frac{\log C_+}{|\mathbf{p}|} \right) \Big] , \quad (3.43)$$

$$\begin{aligned} \mathcal{B} &= \frac{\alpha}{2\pi|\mathbf{p}|^3 E} \int_0^\infty d|\mathbf{k}| \frac{|\mathbf{k}|}{E_k} \left[E_k \left(4|\mathbf{p}|E - 2m_e^2 \log \left(\frac{E + |\mathbf{p}|}{E - |\mathbf{p}|} \right) \right) B(|\mathbf{k}|) + (2|\mathbf{k}||\mathbf{p}|E \right. \\ &- \left. m_e^2(E - E_k) \log C_- \right) F_-(E_k) + (2|\mathbf{k}||\mathbf{p}|E - m_e^2(E + E_k) \log C_+) F_+(E_k) \Big] , \end{aligned} \quad (3.44)$$

The projector on negative energy states reads instead

$$\Lambda_R^- = \frac{\not{p} - m_e^R + \delta_-}{2E} , \quad (3.45)$$

$$\delta_- = (\not{p} - m_e)\mathcal{A} + \left(\not{p} + \frac{|\mathbf{p}|^2}{m_e} \right) \mathcal{B} , \quad (3.46)$$

and $\hat{\mathcal{A}}$ and $\hat{\mathcal{B}}$ can be obtained from \mathcal{A} and \mathcal{B} by replacing $\xi_e \rightarrow -\xi_e$. The contribution due to e^\pm thermal wavefunction renormalization is then obtained by using the thermal renormalized projectors Λ_R^\pm in the evaluation of the Born rate. This procedure, having subtracted the contribution due to the mass renormalization, gives at order α

$$\begin{aligned} \Delta Q_{e^+e^-}^W &= \frac{G_F^2}{12\pi^5} \int_0^\infty d|\mathbf{p}_1| d|\mathbf{p}_2| |\mathbf{p}_1|^2 |\mathbf{p}_2|^2 \left(\frac{1}{E_1} + \frac{1}{E_2} \right) F_-(E_1) F_+(E_2) \\ &\times \left(\left\{ (C_A'^2 + C_V'^2) \left[(E_1 E_2 + m_e^2) (2E_1 E_2 + m_e^2) + \frac{2}{3} |\mathbf{p}_1|^2 |\mathbf{p}_2|^2 \right] \right\} (\mathcal{A}_1 + \hat{\mathcal{A}}_2) \right. \\ &\left. + \frac{2}{3} (C_A'^2 + C_V'^2) |\mathbf{p}_1|^2 |\mathbf{p}_2|^2 (\mathcal{B}_1 + \hat{\mathcal{B}}_2) - 2 (2C_V'^2 - C_A'^2) (E_1 E_2 + m_e^2) (|\mathbf{p}_1|^2 \mathcal{B}_1 + |\mathbf{p}_2|^2 \hat{\mathcal{B}}_2) \right) . \end{aligned} \quad (3.47)$$

The functions $\mathcal{A}_{1,2}$, $\mathcal{B}_{1,2}$, $\hat{\mathcal{A}}_{1,2}$, $\hat{\mathcal{B}}_{1,2}$ are obtained from \mathcal{A} , \mathcal{B} , $\hat{\mathcal{A}}$, $\hat{\mathcal{B}}$ with the substitution $(E, \mathbf{p}) \rightarrow (E_{1,2}, \mathbf{p}_{1,2})$. Again, in the numerical computation of the integrals appearing in the expression for $\Delta Q_{e^+e^-}^W$ we have subtracted all divergent terms.

3.2.2 Vertex renormalization at finite temperature

The lowest order electromagnetic vertex correction to the neutrino energy loss is provided by the interference term between the diagram in Figure 1d and the tree amplitude of Figure 1a. In the amplitude of the vertex diagram, three particle propagators appear, each of them consisting of two terms according to Eqs.(3.16) and (3.17). However, the computation of the thermal vertex renormalization correction to the rate is simplified by 4-momentum conservation arguments. In fact, the mentioned three propagators would produce eight terms in the amplitude, one of which is a pure vacuum term already considered in Sect. 3.1. Three of the remaining terms, proportional to a Fermi-Dirac

distribution function times a Bose-Einstein distribution function, give no contribution to the rate since they correspond to an electromagnetic vertex with a real photon and two real massive particles, which is not allowed by 4-momentum conservation. Moreover, the term proportional to two Fermi functions does not contribute to the interference term with the tree level amplitude since it is purely imaginary. Therefore, we are left with only three terms, one proportional to a Bose-Einstein function and the others proportional to a Fermi-Dirac distribution

$$\Delta Q_{e^+e^-}^V = -\frac{\alpha G_F^2}{48(2\pi)^{10}} \int d^3\mathbf{p}_1 d^3\mathbf{p}_2 d^4k \left(\frac{1}{E_1} + \frac{1}{E_2} \right) F_-(E_1) F_+(E_2) \Phi_V$$

$$\times \left[\frac{\Gamma_B(k)}{[(k+p_1)^2 - m_e^2][(k-p_2)^2 - m_e^2]} - \frac{\Gamma_F(k+p_1)}{[(k-p_2)^2 - m_e^2]k^2} - \frac{\Gamma_F(k-p_2)}{[(k+p_1)^2 - m_e^2]k^2} \right] \quad (3.48)$$

where

$$\begin{aligned} \Phi_V = & 512 C_V'^2 \left[(m_e^2 + p_1 \cdot p_2) \left(-2 p_1 \cdot p_2 (2m_e^2 + p_1 \cdot p_2) - k \cdot p_2 (3m_e^2 + 2 p_1 \cdot p_2) \right. \right. \\ & \left. \left. + k \cdot p_1 (3m_e^2 + 2 k \cdot p_2 + 2 p_1 \cdot p_2) \right) \right] \\ & - 512 C_A'^2 \left[m_e^2 (k \cdot p_1)^2 + m_e^2 (k \cdot p_2)^2 + 2 k \cdot p_2 p_1 \cdot p_2 (m_e^2 + p_1 \cdot p_2) \right. \\ & \left. - 2 k \cdot p_1 p_1 \cdot p_2 (m_e^2 + k \cdot p_2 + p_1 \cdot p_2) + 2 p_1 \cdot p_2 (-m_e^4 + (p_1 \cdot p_2)^2) \right] . \quad (3.49) \end{aligned}$$

The infrared-safe part of these terms (in the limit $k \rightarrow 0$) is obtained by expanding the matrix element function Φ_V in powers of k .

For the Bose-Einstein term (the first one in square brackets in Eq.(3.48)), due to the presence of the function $B(|k_0|)$, one has to subtract from Φ_V the terms in powers of k of order 0 and 1. By choosing the frame where the momentum \mathbf{k} lies along the z -axis and \mathbf{p}_1 is in the x - z plane, denoting with $\theta_{1,2}$ the angle between \mathbf{k} and $\mathbf{p}_{1,2}$ and with ϕ the azimuthal angle of the vector \mathbf{p}_2 , after some algebra one gets

$$\Delta Q_{e^+e^-}^{V,B} = \frac{\alpha G_F^2}{6144 \pi^7} \int_0^\infty d|\mathbf{p}_1| d|\mathbf{p}_2| d|\mathbf{k}| \int_{-1}^1 dx_1 dx_2 |\mathbf{p}_1|^2 |\mathbf{p}_1|^2 |\mathbf{k}| \left(\frac{1}{E_1} + \frac{1}{E_2} \right)$$

$$\times F_-(E_1) F_+(E_2) B(|\mathbf{k}|) I_B , \quad (3.50)$$

where $x_{1,2} = \cos \theta_{1,2}$ and I_B is reported in Appendix A.

The fermionic part (the second and third terms in square brackets in Eq.(3.48)) contains, instead, the expression

$$d^4k \frac{\delta(k^2 + 2k \cdot p_1)}{(k^2 - 2k \cdot p_2)k^2} \Phi_V , \quad (3.51)$$

which, assuming that the integration in dk_0 does not introduce divergent terms, is proportional to

$$d^3\mathbf{k} \frac{\Phi_V}{k \cdot (p_1 + p_2) k \cdot p_1} . \quad (3.52)$$

By using the properties of the δ -function, for $k \rightarrow 0$ we can write

$$\begin{aligned} k_0 &= -E_1 + \sqrt{E_1^2 + |\mathbf{k}|^2 + 2|\mathbf{k}||\mathbf{p}_1|x_1} \\ &\simeq \frac{|\mathbf{p}_1|x_1}{E_1} |\mathbf{k}| + \frac{E_1^2 - |\mathbf{p}_1|^2 x_1}{2E_1^3} |\mathbf{k}|^2 + O(|\mathbf{k}|^3) , \end{aligned} \quad (3.53)$$

and substituting in the expression in (3.52) we find that

$$d^4k \frac{\delta(k^2 + 2k \cdot p_1)}{(k^2 - 2k \cdot p_2)k^2} \Phi_V \sim d|\mathbf{k}| \frac{\Phi_V}{|\mathbf{k}|} . \quad (3.54)$$

Thus, the infrared-safe part of the fermionic term is obtained by subtracting from Φ_V the terms in powers of k of order 0 only. With the same notations as above, after some algebra we get

$$\begin{aligned} \Delta Q_{e^+e^-}^{V,F} &= \frac{\alpha G_F^2}{6144\pi^7} \int_0^\infty d|\mathbf{p}_1| d|\mathbf{p}_2| d|\mathbf{k}| \int_{-1}^1 dx_1 dx_2 \frac{|\mathbf{p}_1|^2 |\mathbf{p}_2|^2 |\mathbf{k}|^2}{E_k} \left(\frac{1}{E_1} + \frac{1}{E_2} \right) \\ &\times F_-(E_1) F_+(E_2) [I_{F_1} F_-(E_k) + I_{F_2} F_+(E_k)] , \end{aligned} \quad (3.55)$$

where $E_k = \sqrt{|\mathbf{k}|^2 + m_e^2}$. The functions $I_{F_{1,2}}$ are defined as follows

$$I_{F_1} = \int_0^{2\pi} d\phi \left[\frac{\tilde{\Phi}_V^{IS}}{[(k - p_1 - p_2)^2 - m_e^2](k - p_1)^2} \Big|_{k_0=E_k} + \frac{\tilde{\Phi}_V^{IS}}{[(k - p_1 - p_2)^2 - m_e^2](k - p_1)^2} \Big|_{k_0=-E_k} \right] , \quad (3.56)$$

$$I_{F_2} = \int_0^{2\pi} d\phi \left[\frac{\hat{\Phi}_V^{IS}}{[(k + p_1 + p_2)^2 - m_e^2](k + p_2)^2} \Big|_{k_0=E_k} + \frac{\hat{\Phi}_V^{IS}}{[(k + p_1 + p_2)^2 - m_e^2](k + p_2)^2} \Big|_{k_0=-E_k} \right] , \quad (3.57)$$

where $\tilde{\Phi}_V^{IS}$ ($\hat{\Phi}_V^{IS}$) is obtained from Φ_V subtracting the terms of order 0 in k and making the substitution $k \rightarrow k - p_1$ ($k \rightarrow k + p_2$). The integrations in Eqs.(3.56), (3.57) may be performed analytically, since they involve integrals of the form

$$I = \int_0^{2\pi} d\phi \frac{n_1 + n_2 \cos \phi + n_3 \cos^2 \phi + n_4 \cos^3 \phi}{d_1 - d_2 \cos \phi} , \quad (3.58)$$

where n_i , d_i do not depend on ϕ . However, since the denominator above may vanish for given values of the momenta involved, the result of the integrations depends on the kinematical region one considers. For each function I_{F_1} and I_{F_2} we distinguish three different cases:

1. $d_2 = 0$:

the integrand functions are just polynomials in $\cos(\phi)$ and no pole is involved:

$$I = \frac{\pi(2n_1 + n_3)}{d_1} ; \quad (3.59)$$

2. $d_2 \neq 0$, $\left|\frac{d_1}{d_2}\right| \geq 1$:

inside the integration region in ϕ no pole may occur and the result is

$$I = -2\pi \left[\frac{n_2}{d_2} + \frac{n_4}{2d_2} + \frac{d_1 n_3}{d_2^2} + \frac{d_1^2 n_4}{d_2^3} - \sqrt{\frac{d_1 + d_2}{d_1 - d_2}} \frac{1}{d_1 + d_2} \left(n_1 + \frac{d_1 n_2}{d_2} + \frac{d_1^2 n_3}{d_2^2} + \frac{d_1^3 n_4}{d_2^3} \right) \right] ; \quad (3.60)$$

3. $d_2 \neq 0$, $\left|\frac{d_1}{d_2}\right| < 1$:

in this case the integrand function may develop a pole and the integral I has to be evaluated in the principal value sense:

$$I = \frac{-\pi [2d_1 d_2 n_3 + 2d_1^2 n_4 + d_2^2 (2n_2 + n_4)]}{d_2^3} . \quad (3.61)$$

The final expressions of the functions $I_{F_{1,2}}$ are reported in Appendix A. Thus, the thermal vertex renormalization correction to neutrino energy loss rate due to pair annihilations reads

$$\Delta Q_{e^+e^-}^V = \Delta Q_{e^+e^-}^{V,B} + \Delta Q_{e^+e^-}^{V,F} . \quad (3.62)$$

3.2.3 Bremsstrahlung: γ emission/absorption

As stated above, in order to eliminate the infrared divergencies present in the radiative diagrams of Figures 1b–1d it is necessary to include the rates of processes where a photon is either absorbed or emitted (see Figures 1e–1h). The energy loss rates due to γ emission (absorption) $\Delta Q_{e^+e^-}^{E(A)}$, are given by the sum of squared amplitudes of the processes of Figures 1e–1h, namely

$$\begin{aligned} \Delta Q_{e^+e^-}^E &= \frac{1}{(2\pi)^9} \int \frac{d^3\mathbf{p}_1}{2E_1} \int \frac{d^3\mathbf{p}_2}{2E_2} \int \frac{d^3\mathbf{k}}{2|\mathbf{k}|} (E_1 + E_2 - |\mathbf{k}|) F_-(E_1) F_+(E_2) [1 + B(|\mathbf{k}|)] \\ &\times \left\{ \frac{1}{(2\pi)^2} \int \frac{d^3\mathbf{q}_1}{2\omega_1} \int \frac{d^3\mathbf{q}_2}{2\omega_2} \delta^4(p_1 + p_2 - q_1 - q_2 - k) \sum_{spin,\alpha} |M_{e^+e^- \rightarrow \nu_\alpha \bar{\nu}_\alpha \gamma}|^2 \right\}, \end{aligned} \quad (3.63)$$

$$\begin{aligned}
\Delta Q_{e^+e^-}^A &= \frac{1}{(2\pi)^9} \int \frac{d^3\mathbf{p}_1}{2E_1} \int \frac{d^3\mathbf{p}_2}{2E_2} \int \frac{d^3\mathbf{k}}{2|\mathbf{k}|} (E_1 + E_2 + |\mathbf{k}|) F_-(E_1) F_+(E_2) B(|\mathbf{k}|) \\
&\times \left\{ \frac{1}{(2\pi)^2} \int \frac{d^3\mathbf{q}_1}{2\omega_1} \int \frac{d^3\mathbf{q}_2}{2\omega_2} \delta^4(p_1 + p_2 - q_1 - q_2 + k) \sum_{spin,\alpha} |M_{e^+e^- \gamma \rightarrow \nu_\alpha \bar{\nu}_\alpha}|^2 \right\}.
\end{aligned} \tag{3.64}$$

Note that in the computation of the amplitudes for both processes, only the vacuum part of the electron or positron propagator should enter since, otherwise, we would have an electromagnetic vertex with a real photon and two real electrons or positrons which is not allowed by 4-momentum conservation.

The term proportional to unity in the statistical factor $(1+B(|\mathbf{k}|))$ entering in Eq.(3.63) is responsible for the spontaneous emission in vacuum. For small $|\mathbf{k}|$ this contribution has been already discussed in Section 3.1 (Soft-Bremsstrahlung), hence we have to consider only the hard-photon emission part corresponding to photon energies above the introduced cutoff ϵ .

For the γ emission, the term in curly brackets in Eq.(3.63) is given by

$$\begin{aligned}
\Phi^E &= \frac{\alpha G_F^2}{24} \Theta(E_1 + E_2 - |\mathbf{k}|) \Theta(m_e^2 + p_1 \cdot p_2 - k \cdot (p_1 + p_2)) \\
&\times \left[\frac{\Phi_1^E}{(p_1 \cdot k)^2} + \frac{\Phi_2^E}{(p_2 \cdot k)^2} + \frac{\Phi_{12}^E}{(p_1 \cdot k)(p_2 \cdot k)} \right],
\end{aligned} \tag{3.65}$$

while for γ absorption we have

$$\Phi^A = \frac{\alpha G_F^2}{24} \left[\frac{\Phi_1^A}{(p_1 \cdot k)^2} + \frac{\Phi_2^A}{(p_2 \cdot k)^2} + \frac{\Phi_{12}^A}{(p_1 \cdot k)(p_2 \cdot k)} \right]. \tag{3.66}$$

The functions Φ_1^E , Φ_2^E , Φ_{12}^E are reported in Appendix B while Φ_1^A , Φ_2^A , Φ_{12}^A for the photon absorption are obtained from the corresponding Φ_i^E by simply replacing the 4-momentum k with $-k$. The Θ -functions appearing in Eq.(3.65), coming from the Lenard formula used in performing neutrino momentum integration, give the kinematical conditions for the process to occur. Obviously, for the γ absorption we have no kinematical constraints and we have omitted the superfluous Θ -functions ².

In the limit $|\mathbf{k}| \rightarrow 0$ the integrand function in Eq.(3.63) (where the expression in Eq.(3.65) has been substituted) shows some divergences which cancel the corresponding

²In this case the arguments of the Θ -functions are always positive for all values of the particle 4-momenta, as it can be easily checked, for example, in the electron-positron center of mass frame.

infrared singularities in the radiative corrections considered previously. To pick up the divergent terms, we note that the relevant expression appearing in $\Delta Q_{e^+e^-}^E$ is the following:

$$\frac{|\mathbf{k}|^2}{|\mathbf{k}|} (E_1 + E_2 - |\mathbf{k}|) \Phi^E [1 + B(|\mathbf{k}|)] . \quad (3.67)$$

Thus, by expanding Φ^E in powers of $|\mathbf{k}|$, the infrared-safe part is obtained by subtracting the terms up to order 0 in $|\mathbf{k}|$ to the expression proportional to the Bose function. As far as the factor which does not contain $B(|\mathbf{k}|)$ is concerned, we observe that no change has to be performed because we must integrate this term for $|\mathbf{k}|$ ranging from the cutoff ϵ to the infinity, since the soft part of the (vacuum) bremsstrahlung has been already considered in Section 3.1.

Analogous divergent terms for $|\mathbf{k}| \rightarrow 0$ appear in the integrand function for the energy loss induced by photon absorption. In this case the relevant expression to be considered is

$$\frac{|\mathbf{k}|^2}{|\mathbf{k}|} (E_1 + E_2 + |\mathbf{k}|) \Phi^A B(|\mathbf{k}|) , \quad (3.68)$$

and, as in the previous case, the infrared-safe part is obtained by subtracting terms up to order 0 in $|\mathbf{k}|$.

Finally, the integrations in the electron, positron and photon 3-momenta in Eq.(3.63) must be performed by taking into account the Θ -functions in Eq.(3.65). We choose the frame where the photon momentum \mathbf{k} lies along the z -axis and \mathbf{p}_1 is in the x - z plane. We also denote with $\theta_{1,2}$ the angle between \mathbf{k} and $\mathbf{p}_{1,2}$ and with ϕ the azimuthal angle of the vector \mathbf{p}_2 .

The kinematical constraints can be implemented as follows. The integration range for the variables $|\mathbf{p}_1|$, $|\mathbf{p}_2|$ is not limited (they run over the entire $[0, \infty[$ interval), as well as those for θ_1 , θ_2 (ranging from 0 to π). The integration in the modulus of the photon momentum $|\mathbf{k}|$ is bound to the region $|\mathbf{k}| \leq E_1 + E_2$, thus implementing the condition coming from the first Θ -function in Eq.(3.65). The remaining kinematical constraint can be written as:

$$a_1 \cos \phi \leq a_2 , \quad (3.69)$$

with $(s_{1,2} = \sin \theta_{1,2}, x_{1,2} = \cos \theta_{1,2})$

$$a_1 = |\mathbf{p}_1| |\mathbf{p}_2| s_1 s_2 , \quad (3.70)$$

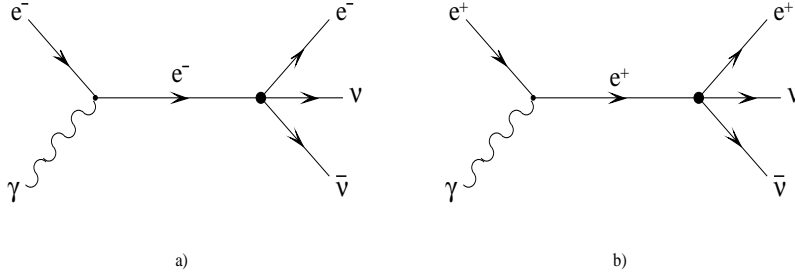


Figure 3: Feynman diagrams for the neutrino photoproduction processes.

$$a_2 = E_1 E_2 - |\mathbf{p}_1| |\mathbf{p}_2| x_1 x_2 - |\mathbf{k}| (E_1 + E_2 - |\mathbf{p}_1| x_1 - |\mathbf{p}_2| x_2) + m_e^2 . \quad (3.71)$$

This gives no effective condition when $a_1 = 0$, $a_2 \geq 0$ or $a_1 \neq 0$, $a_2/a_1 \geq 1$, thus leaving the integration over ϕ ranging from 0 to 2π , while Eq.(3.69) cannot be fulfilled when $a_1 = 0$, $a_2 < 0$ or $a_1 \neq 0$, $a_2/a_1 \leq -1$, thus resulting in $\Delta Q_{e^+e^-}^E = 0$ for these cases. In the remaining cases, that is $a_1 \neq 0$, $-1 < a_2/a_1 < 1$, the integration interval in ϕ is $[\alpha, 2\pi - \alpha]$ with $\alpha = \arccos(a_2/a_1)$.

For the photon absorption case, since there are no kinematical constraints, the integration on $|\mathbf{k}|$ as well as on the angle ϕ is not restricted to a given region but ranges over all possible values.

The final expression for the sum of the neutrino energy loss rate induced by photon emission and absorption is the following:

$$\begin{aligned} \Delta Q_{e^+e^-}^E + \Delta Q_{e^+e^-}^A &= \frac{\alpha G_F^2}{3072 \pi^7} \int d|\mathbf{p}_1| d|\mathbf{p}_2| d|\mathbf{k}| dx_1 dx_2 \frac{|\mathbf{p}_1|^2 |\mathbf{p}_2|^2}{E_1 E_2} F_-(E_1) F_+(E_2) \\ &\quad \times [I_{e0} \Theta(E_1 + E_2 - |\mathbf{k}|) + (I_e \Theta(E_1 + E_2 - |\mathbf{k}|) + I_a) B(|\mathbf{k}|)] , \quad (3.72) \end{aligned}$$

where the function I_{e0}, I_e, I_a are reported in Appendix B.

4 Neutrino photoproduction

Neutrino photoproduction processes $\gamma(k) + e^\pm(p_1) \rightarrow e^\pm(p_2) + \nu_\alpha(q_1) + \bar{\nu}_\alpha(q_2)$ contribute to the neutrino energy loss rate, at the same perturbative order as the electromagnetic corrections to the pair annihilation process. Thus, they must be included in a comprehensive study of the star cooling rate. The relevant diagrams for photoproduction on e^- or e^+ , shown in Figure 3, are simply obtained by crossing the corresponding ones for photon

absorption in Figures 1g, 1h, and the neutrino energy loss rates take the following forms

$$\begin{aligned}
Q_{\gamma e^-} &= \frac{1}{(2\pi)^9} \int \frac{d^3\mathbf{p}_1}{2E_1} \int \frac{d^3\mathbf{p}_2}{2E_2} \int \frac{d^3\mathbf{k}}{2E_\gamma} (E_1 - E_2 + E_\gamma) F_-(E_1) [1 - F_-(E_2)] B(E_\gamma) \\
&\times \left\{ \frac{1}{(2\pi)^2} \int \frac{d^3\mathbf{q}_1}{2\omega_1} \int \frac{d^3\mathbf{q}_2}{2\omega_2} \delta^4(k + p_1 - p_2 - q_1 - q_2) \sum_{spin,\alpha} |M_{\gamma e^- \rightarrow e^- \nu_\alpha \bar{\nu}_\alpha}|^2 \right\}, \tag{4.73}
\end{aligned}$$

$$\begin{aligned}
Q_{\gamma e^+} &= \frac{1}{(2\pi)^9} \int \frac{d^3\mathbf{p}_1}{2E_1} \int \frac{d^3\mathbf{p}_2}{2E_2} \int \frac{d^3\mathbf{k}}{2E_\gamma} (E_2 - E_1 + E_\gamma) F_+(E_2) [1 - F_+(E_1)] B(E_\gamma) \\
&\times \left\{ \frac{1}{(2\pi)^2} \int \frac{d^3\mathbf{q}_1}{2\omega_1} \int \frac{d^3\mathbf{q}_2}{2\omega_2} \delta^4(k + p_2 - p_1 - q_1 - q_2) \sum_{spin,\alpha} |M_{\gamma e^+ \rightarrow e^+ \nu_\alpha \bar{\nu}_\alpha}|^2 \right\}. \tag{4.74}
\end{aligned}$$

Differently from what happens for the corrections to the pair process, analyzed in the previous Section, in the calculations of photoproduction rates we must take into account the photon effective mass m_γ depending on the density and temperature of the plasma. This effect could be neglected in all the $e^+e^- \rightarrow \nu\bar{\nu}$ radiative corrections because it yielded an irrelevant change in the neutrino energy loss rate, but it is important for the photoproduction processes which exhibit a strong dependence on the background density in the high density region.

In the following we consider a *massive* photon with the following renormalized mass [27]

$$m_\gamma^2 = \frac{4\alpha}{\pi} \int_0^\infty d|\mathbf{k}| \frac{|\mathbf{k}|^2}{E_k} (F_+(E_k) + F_-(E_k)) , \tag{4.75}$$

where we have adopted the same notations of Eq.(3.34) and the completeness relation

$$\sum_\lambda \epsilon_\mu^{(\lambda)} \epsilon_\nu^{(\lambda)} = -g_{\mu\nu} + \frac{k_\mu k_\nu}{k^2} . \tag{4.76}$$

Note that a finite photon mass eliminates infrared divergencies due to the Bose distribution function in the rates. For the sake of brevity, in the following we describe the calculations for photoproduction on electron only. The corresponding ones for photoproduction on positron can be obtained by replacing $\xi_e \rightarrow -\xi_e$.

The term in curly brackets in Eq.(4.73) is given by

$$\begin{aligned}
\Phi_{ph} &= \frac{8\alpha G_F^2}{3m_\gamma^2} \Theta(E_1 - E_2 + E_\gamma) \Theta(2m_e^2 + m_\gamma^2 - 2p_1 \cdot p_2 + 2k \cdot (p_1 - p_2)) \\
&\times \left[\frac{\Phi_{ph}^1}{(m_\gamma^2 + 2p_1 \cdot k)^2} + \frac{\Phi_{ph}^2}{(m_\gamma^2 - 2p_2 \cdot k)^2} + \frac{2\Phi_{ph}^{12}}{(m_\gamma^2 + 2p_1 \cdot k)(m_\gamma^2 - 2p_2 \cdot k)} \right] \tag{4.77}
\end{aligned}$$

The squared amplitude function Φ_{ph}^1 , Φ_{ph}^2 , Φ_{ph}^{12} , are reported in Appendix C. The Θ -functions appearing in Eq.(4.77), coming from the Lenard formula used in performing neutrino momentum integration, give the kinematical conditions for the process to occur. The remaining integrations on the incoming electron and photon and outgoing electron 3-momenta in Eq.(4.73) are performed, in close analogy to what done in Section 3.2.3, by choosing the frame where the photon momentum \mathbf{k} lies along the z -axis and \mathbf{p}_1 is in the x - z plane (denoting with $\theta_{1,2}$ the angle between \mathbf{k} and $\mathbf{p}_{1,2}$ and with ϕ the azimuthal angle of the vector \mathbf{p}_2). In particular the integration in $|\mathbf{p}_1|$, $|\mathbf{k}|$, θ_1 , θ_2 ranges over all possible values for these variables, while the integration field for $|\mathbf{p}_2|$ is limited by the first Θ -function in Eq.(4.77):

$$0 \leq |\mathbf{p}_2| \leq \sqrt{|\mathbf{p}_1|^2 + E_\gamma^2 + 2E_\gamma E_1} \equiv p_2^{max} . \quad (4.78)$$

The remaining kinematical constraint, which has to be used to perform the integration on the angle ϕ , can be written as:

$$b_1 \cos \phi \geq b_2 , \quad (4.79)$$

with ($s_{1,2} = \sin \theta_{1,2}$, $x_{1,2} = \cos \theta_{1,2}$)

$$b_1 = 2 |\mathbf{p}_1| |\mathbf{p}_2| s_1 s_2 , \quad (4.80)$$

$$b_2 = 2 E_1 E_2 - 2 |\mathbf{p}_1| |\mathbf{p}_2| x_1 x_2 - 2 E_\gamma (E_1 - E_2) + \\ + 2 |\mathbf{k}| (|\mathbf{p}_1| x_1 - |\mathbf{p}_2| x_2) - 2 m_e^2 - m_\gamma^2 . \quad (4.81)$$

Note that the condition (4.79) is not fulfilled when $b_1 = 0$, $b_2 > 0$ or $b_1 \neq 0$, $b_2/b_1 \geq 1$, thus resulting in $Q_{\gamma e^-} = 0$, while it is trivially realized for $b_1 = 0$, $b_2 \leq 0$, where case the integration field for ϕ is $[0, 2\pi]$. The constraint (4.79) can be non trivially satisfied only for $b_1 \neq 0$, $-1 < b_2/b_1 < 1$, when the integration region for ϕ is $[0, \beta] \cup [2\pi - \beta, 2\pi]$ with $\beta = \arccos(b_2/b_1)$. The final expression for the energy loss rate induced by neutrino photoproduction on electron is the following

$$Q_{\gamma e^-} = \frac{\alpha G_F^2}{3072 \pi^7} \int_0^\infty d|\mathbf{p}_1| d|\mathbf{k}| \int_0^{p_2^{max}} d|\mathbf{p}_2| \int_{-1}^1 dx_1 dx_2 \frac{|\mathbf{p}_1|^2 |\mathbf{p}_2|^2}{E_1 E_2} \\ \times F_-(E_1) [1 - F_-(E_2)] B(E_\gamma) I_{ph} , \quad (4.82)$$

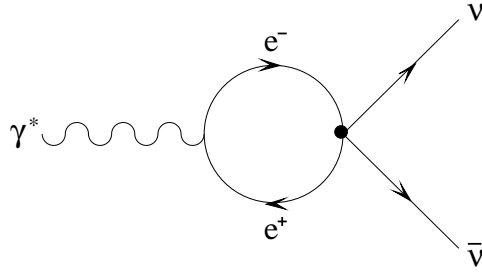


Figure 4: Feynman diagram for the plasmon decay into a neutrino-antineutrino pair.

where the function I_{ph} is reported in Appendix C.

The corresponding expression for the rate induced by neutrino photoproduction on positron is easily obtained from Eq.(4.82) with simple substitutions,

$$\begin{aligned}
 Q_{\gamma e^+} &= \frac{\alpha G_F^2}{3072 \pi^7} \int_0^\infty d|\mathbf{p}_2| d|\mathbf{k}| \int_0^{p_1^{\max}} d|\mathbf{p}_1| \int_{-1}^1 dx_1 dx_2 \frac{|\mathbf{p}_1|^2 |\mathbf{p}_2|^2}{E_1 E_2} \\
 &\times F_+(E_2) [1 - F_+(E_1)] B(E_\gamma) I'_{ph} \ , \tag{4.83}
 \end{aligned}$$

and I'_{ph} is obtained from I_{ph} with $p_1 \leftrightarrow p_2$ ³. Thus by using the expressions (4.82) and (4.83), one gets the total energy loss rate due to neutrino photoproduction as

$$Q_{\gamma e} = Q_{\gamma e^-} + Q_{\gamma e^+} \ . \tag{4.84}$$

5 Plasmon decay

The plasma process $\gamma^*(k) \rightarrow \nu_\alpha(q_1) + \bar{\nu}_\alpha(q_2)$ is of higher order in α with respect to the pair annihilation process (it is of order $\alpha\sqrt{\alpha}G_F^2$) but, nevertheless, its contribution to neutrino energy loss rate is dominant for a wide region of stellar temperatures and densities [21]. Then, in this Section, we discuss this process and evaluate the corresponding energy loss rate.

The decay $\gamma^* \rightarrow \nu_\alpha + \bar{\nu}_\alpha$ takes place only if the photon momentum is a time-like 4-vector such that $E_\gamma > |\mathbf{k}|$. To see when this constraint applies, we have first to calculate the dispersion relation for a photon in a thermal plasma and this is recalled in Appendix D. For transverse (T) propagation modes there is no effective constraint, while for longitudinal (L) ones the decay occurs only for $|\mathbf{k}| < |\mathbf{k}|_{\max}$, where $|\mathbf{k}|_{\max}$ is the maximum

³Note that the kinematics of the process is the same as for the photoproduction on electron by replacing the 4-vector p_1 with p_2 .

plasmon momentum in the bath whose expression is reported in Appendix D.

At lowest order the process $\gamma^* \rightarrow \nu_\alpha + \bar{\nu}_\alpha$ is described by the Feynman diagram in Fig. 4 and the loss rate is given by

$$Q_{\gamma^*} = Q_{\gamma^*}^L + Q_{\gamma^*}^T , \quad (5.85)$$

where the partial rates

$$\begin{aligned} Q_{\gamma^*}^{L,T} &= \frac{1}{(2\pi)^3} \int \frac{d^3\mathbf{k}}{2E_{\gamma L,T}} E_{\gamma L,T} B(E_{\gamma L,T}) \\ &\times \left\{ \frac{1}{(2\pi)^2} \int \frac{d^3\mathbf{q}_1}{2\omega_1} \int \frac{d^3\mathbf{q}_2}{2\omega_2} \delta^4(k - q_1 - q_2) \sum_\alpha |M_{\gamma^* \rightarrow \nu_\alpha \bar{\nu}_\alpha}^{L,T}|^2 \right\} , \end{aligned} \quad (5.86)$$

correspond to longitudinal and transverse photon mode propagation, respectively. The computation of the invariant amplitude for the considered decay can proceed through an effective photon-neutrino interaction

$$M_{\gamma^* \rightarrow \nu \bar{\nu}}^\lambda = \bar{u}(q_1) \gamma^\mu (1 - \gamma_5) v(q_2) \Gamma_{\alpha\mu}(k) \epsilon_\lambda^\alpha(k) , \quad (5.87)$$

where $\epsilon_\lambda^\alpha(k)$ is the polarization 4-vector for longitudinal ($\lambda = L$) or transverse ($\lambda = T$) thermal photons and, by considering only the thermal on-shell propagation of e^\pm in the loop in Figure 4. Thus one gets

$$\Gamma_{\alpha\mu}(k) = i \frac{eG_F}{\sqrt{2}} \int \frac{d^4p}{(2\pi)^4} [C_V' S_{\alpha\mu} - iC_A' A_{\alpha\mu}] \left[\frac{\Gamma_F(p-k)}{p^2 - m_e^2} + \frac{\Gamma_F(p)}{(p-k)^2 - m_e^2} \right] \quad (5.88)$$

$$S_{\alpha\mu} = (p-k)_\alpha p_\mu + (p-k)_\mu p_\alpha + p \cdot k g_{\alpha\mu} , \quad (5.89)$$

$$A_{\alpha\mu} = \epsilon_{\alpha\mu\rho\sigma} k^\rho p^\sigma . \quad (5.90)$$

The quantity in curly brackets in Eq.(5.86) is thus given by [19]:

$$\Phi_{\gamma^*}^{L,T} = -\frac{(E_{\gamma L,T})^2 - k^2}{3\pi} g_{\mu\nu} P_{L,T}^{\mu\nu} , \quad (5.91)$$

$$P_L^{\mu\nu} = -Z_L Q_{\alpha\beta} \Gamma^{\alpha\mu} (\Gamma^{\beta\nu})^* , \quad (5.92)$$

$$P_T^{\mu\nu} = -2Z_T R_{\alpha\beta} \Gamma^{\alpha\mu} (\Gamma^{\beta\nu})^* , \quad (5.93)$$

$$Q^{\alpha\beta} = \frac{K^2}{K^2 - (u \cdot K)^2} \left(u^\alpha - \frac{u \cdot K}{K^2} K^\alpha \right) \left(u^\beta - \frac{u \cdot K}{K^2} K^\beta \right) , \quad (5.94)$$

$$R^{\alpha\beta} = g^{\alpha\beta} - \frac{K^\alpha K^\beta}{K^2} - Q^{\alpha\beta} , \quad (5.95)$$

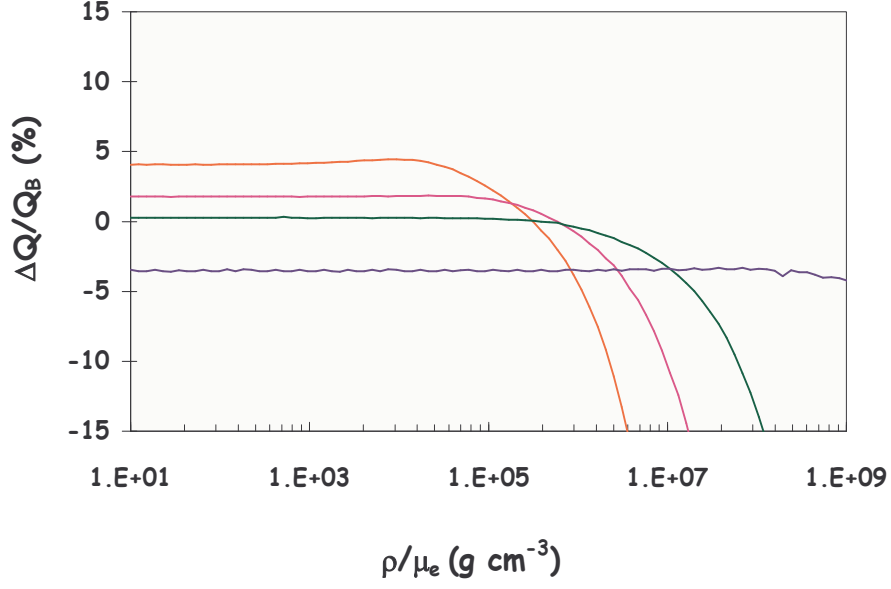


Figure 5: The total radiative corrections normalized to the Born approximation result for the pair annihilation process for $T = 10^8, 10^{8.5}, 10^9, 10^{10}$ °K (from top to bottom).

where $u^\alpha = (1, \mathbf{0})$ is the medium 4-velocity and we have used the orthogonality condition $K_\alpha \Gamma^{\alpha\mu} = 0$, with $K = (E_\gamma, \mathbf{k})$ and $E_\gamma = \sqrt{|\mathbf{k}|^2 + m_\gamma^2}$. Note that for longitudinal and transverse photon modes in a plasma we have [28, 19]

$$\sum_{\lambda=0} \epsilon_\lambda^\alpha \epsilon_\lambda^{\beta*} = -Q^{\alpha\beta} Z_L, \quad (5.96)$$

$$\sum_{\lambda=\pm 1} \epsilon_\lambda^\alpha \epsilon_\lambda^{\beta*} = -2R^{\alpha\beta} Z_T, \quad (5.97)$$

respectively, where the k -dependent functions $Z_{L,T}$ can be found in Appendix D. The energy loss rates are, then [19, 21]

$$Q_{\gamma^*}^L = \frac{G_F^2 C_V'^2}{96\pi^4 \alpha} \int_0^{|\mathbf{k}|_{\max}} d|\mathbf{k}| |\mathbf{k}|^2 B(E_{\gamma L}) Z_L \Pi_L^3, \quad (5.98)$$

$$Q_{\gamma^*}^T = \frac{G_F^2 C_V'^2}{48\pi^4 \alpha} \int_0^\infty d|\mathbf{k}| |\mathbf{k}|^2 B(E_{\gamma T}) Z_T \Pi_T^3, \quad (5.99)$$

with $\Pi_{L,T}$ reported in Appendix D.

6 Results and conclusions

In this paper we have presented an exhaustive computation of the energy loss rates in neutrinos of the stellar interior. A consistent analysis of all leptonic processes up to order

α in the electromagnetic fine structure constant has been performed: neutrino energy loss rate due to pair annihilations, evaluated in Born approximation, $Q_{e^+e^-}^B$ (2.12), has been corrected including both *vacuum* and *thermal* radiative corrections, the latter being computed in the real time formalism. By using Eqs.(2.1), (2.12), (3.33), (3.36), (3.48), (3.62), and (3.72), the total radiative correction $\Delta Q_{e^+e^-}$ results

$$\begin{aligned} \Delta Q_{e^+e^-} &\equiv Q_{e^+e^-} - Q_{e^+e^-}^B \\ &= \Delta Q_{e^+e^-}^{T=0} + \Delta Q_{e^+e^-}^M + \Delta Q_{e^+e^-}^W + \Delta Q_{e^+e^-}^V + \Delta Q_{e^+e^-}^E + \Delta Q_{e^+e^-}^A . \end{aligned} \quad (6.100)$$

In Figure 5, we plot the ratio $\Delta Q_{e^+e^-}/Q_{e^+e^-}^B$ as functions of the plasma density for some values of the temperature, namely $T = 10^8, 10^{8.5}, 10^9, 10^{10} \text{ }^\circ K$. The corrections are found to be of the order of few percent and negative for high temperatures, implying that for these temperatures the energy loss is sensibly decreased. For fixed temperature, $\Delta Q_{e^+e^-}/Q_{e^+e^-}^B$ goes to a constant value for low density. This can be easily understood, since in this limit the plasma is weakly degenerate, and therefore the energy loss rate depends on temperature only. At large densities the ratio $\Delta Q_{e^+e^-}/Q_{e^+e^-}^B$ decreases and reaches larger negative values. However, for such high densities the pair annihilation rates are exceedingly small and thus this process gives only a marginal contribution to the star cooling.

In order to perform a comprehensive study, we have also recalculated the contribution from ν -photoproduction and plasmon decay processes. The corresponding numerical results are presented in Figure 6, where we show the several contributions to total neutrino energy loss rate. When possible, we also show for comparison the results of Ref. [22]. In particular we find a fair agreement with the results reported in literature. For completeness we also show the energy loss rate due to bremsstrahlung on nuclei, denoted with Q_{eZ} , which have been produced using the analytic fitting formula of Ref. [22].

In summary, Figure 6 shows that, as well known, for large temperatures and not too high densities, pair annihilation dominates over the other three processes, while for low densities ν -photoproduction dominates over plasmon decay and bremsstrahlung on nuclei. On the other hand, for large densities the most relevant process is plasmon decay, whose rate however, along with those of all other processes, rapidly falls down for extremely

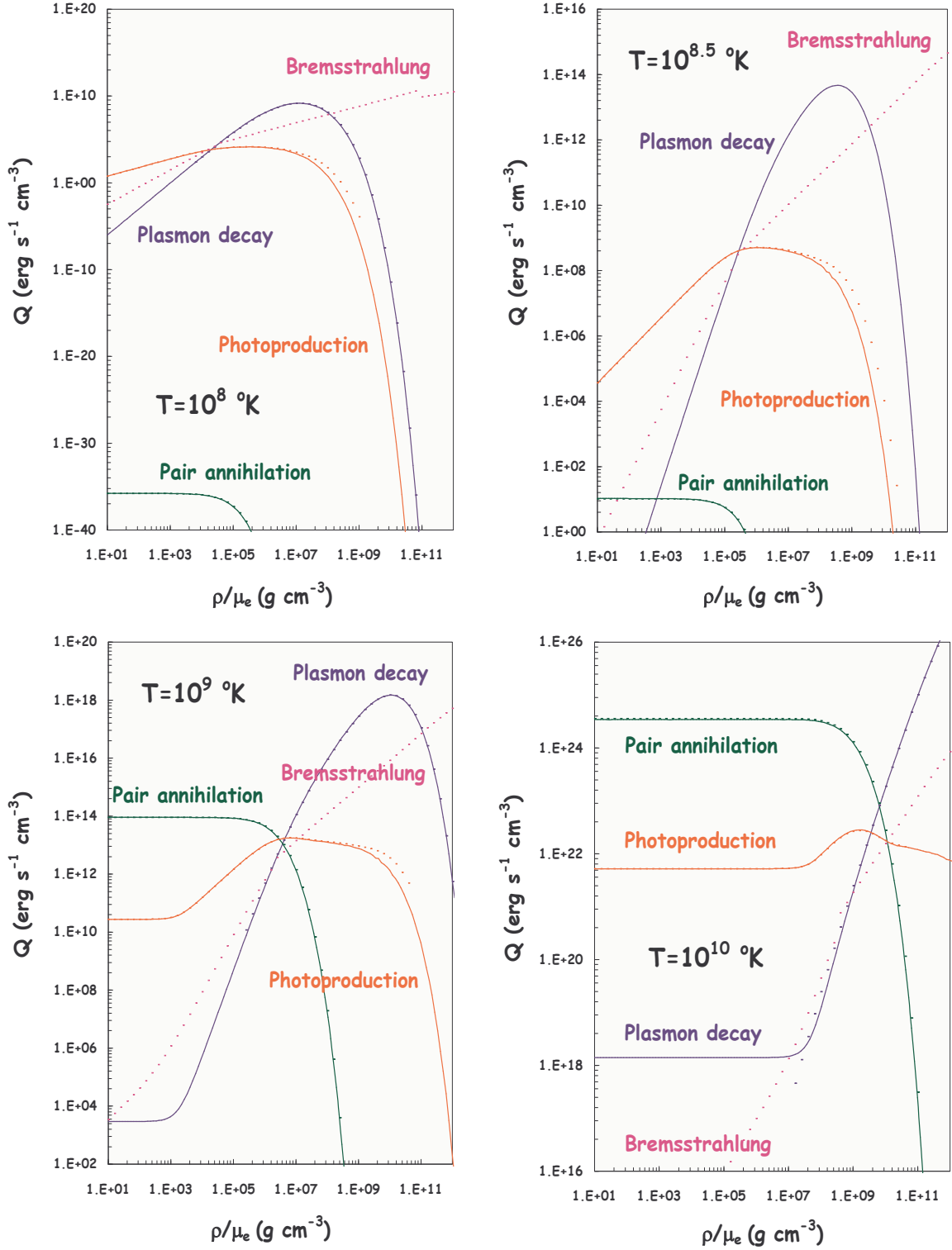


Figure 6: The energy loss rate versus ρ/μ_e due to pair annihilation including radiative corrections $Q_{e^+e^-}$, photoproduction $Q_{\gamma e}$ and plasmon decay Q_{γ^*} (solid lines) for several temperatures (see for definitions Eqs.(2.1), (4.84), (5.85)). The dotted lines refer to the analogous results of Ref. [22], where the rate for bremsstrahlung on nuclei is also computed. The effect of $\Delta Q_{e^+e^-}$ to pair annihilation cannot be appreciated in this logarithmic scale but for the largest temperature $10^{10} \text{ }^\circ\text{K}$.

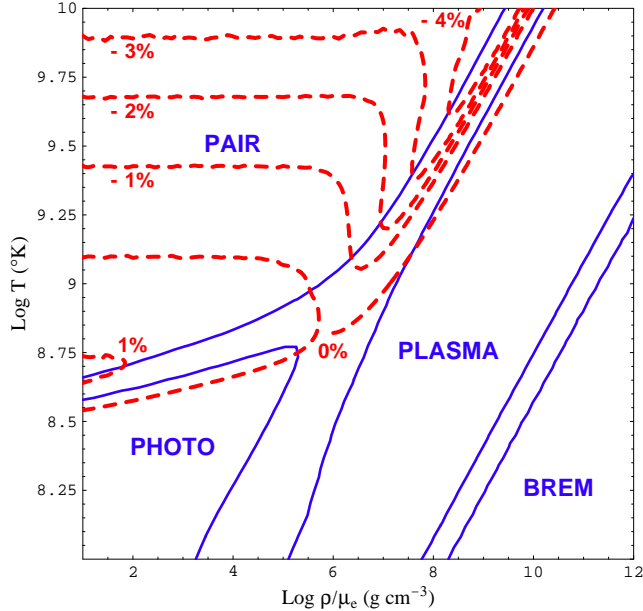


Figure 7: The regions in the $T - \rho/\mu_e$ plane where each of the processes i)-iv) contribute for more than 90% to the total energy loss rate. We also show the contours for the relative correction $\Delta Q/Q_{Tot}^0$ (see text) for the values 1%, 0%, -1%, -2%, -3%, -4%.

high densities. This is a genuine plasma effect as noted in [23]. Consider, for example, the behaviour of ν -photoproduction energy loss. As already noted in [3], the decrease for very large densities is achieved only if one consistently takes into account the increasingly large photon thermal mass. In fact with a massless photon the ν -photoproduction curves in Figure 6 would rather reach a constant value. The main effect of m_γ^2 is a lowering of the values of the Bose distribution function for photons, i.e. a smaller number of thermal photons. This reduces the energy loss rate induced by ν -photoproduction.

In Figure 7 we show the regions in the temperature-density plane where a given process contributes to the total energy loss rate $Q_{Tot} = Q_{e^+e^-} + Q_{\gamma e} + Q_{\gamma^*} + Q_{eZ}$ (including radiative corrections to pair annihilation) for more than 90%. We also summarize there our results on the radiative corrections to pair annihilation processes, by plotting the contours corresponding to $\Delta Q_{e^+e^-}/Q_{Tot}^0 = 1\%, 0\%, -1\%, -2\%, -3\%, -4\%$, where Q_{Tot}^0 is the total emission rate with pair annihilation calculated in Born approximation. These contours lie almost entirely in the region where the pair annihilation process gives the main contribution to the total energy loss rate. This result may affect the late stages of

evolution of very massive stars by changing their configuration at the onset of Supernova explosion.

Acknowledgements

The authors would like to thank S. Chieffi, G. Imbriani, M. Limongi, M. Passera, O. Straniero for useful discussions and comments.

A Vertex correction functions

With the same notations of Section 3.2.2, the function I_B appearing in Eq.(3.50) is given by:

$$\begin{aligned}
I_B &= \frac{1}{4} \int_0^{2\pi} d\phi \left[\frac{\Phi_V^{IS}}{p_1 \cdot k p_2 \cdot k} \Big|_{k_0=|\mathbf{k}|} + \frac{\Phi_V^{IS}}{p_1 \cdot k p_2 \cdot k} \Big|_{k_0=-|\mathbf{k}|} \right] \\
&= 256 C_A'^2 \pi \left(2 E_1 E_2 - 2 |\mathbf{p}_1| |\mathbf{p}_2| x_1 x_2 - m_e^2 \frac{E_1 - |\mathbf{p}_1| x_1}{E_2 - |\mathbf{p}_2| x_2} - m_e^2 \frac{E_2 - |\mathbf{p}_2| x_2}{E_1 - |\mathbf{p}_1| x_1} \right) \\
&\quad + 512 C_V'^2 \pi \left(m_e^2 + E_1 E_2 - |\mathbf{p}_1| |\mathbf{p}_2| x_1 x_2 \right) , \tag{A.1}
\end{aligned}$$

where Φ_V^{IS} is Φ_V once subtracted the terms of order 0 and 1 in k .

On the other side, after performing the integration involved in Eq.(3.58), one obtains in the three cases of Section 3.2.2:

1. $d_2 = 0$;

$$\begin{aligned}
I_{F_1} &= \frac{-128 \pi}{(m_e^2 - k \cdot p_1) [k \cdot (p_1 + p_2) - E_1 E_2 - m_e^2 + |\mathbf{p}_1| |\mathbf{p}_2| x_1 x_2]} \\
&\times \left\{ C_V'^2 [|\mathbf{p}_1|^2 |\mathbf{p}_2|^2 (-1 + x_1^2) (-1 + x_2^2)] \right. \\
&\times \left(6 E_1 E_2 - 2 k \cdot p_2 + 5 m_e^2 - 6 |\mathbf{p}_1| |\mathbf{p}_2| x_1 x_2 \right) \\
&+ 2 \left(E_1 E_2 + m_e^2 - |\mathbf{p}_1| |\mathbf{p}_2| x_1 x_2 \right) \left(2 E_1^2 E_2^2 - 5 k \cdot p_2 m_e^2 \right. \\
&+ k \cdot p_1 \left(2 k \cdot p_2 + 3 m_e^2 \right) - 3 m_e^4 - 3 m_e^2 |\mathbf{p}_1| |\mathbf{p}_2| x_1 x_2 \\
&+ E_1 E_2 \left(-2 k \cdot p_2 + 3 m_e^2 - 4 |\mathbf{p}_1| |\mathbf{p}_2| x_1 x_2 \right) \\
&+ \left. \left. 2 |\mathbf{p}_1| |\mathbf{p}_2| x_1 x_2 (k \cdot p_2 + |\mathbf{p}_1| |\mathbf{p}_2| x_1 x_2) \right) \right] \\
&+ C_A'^2 [|\mathbf{p}_1|^2 |\mathbf{p}_2|^2 (-1 + x_1^2) (-1 + x_2^2)] \\
&\times \left(6 E_1 E_2 - 2 k \cdot p_2 + m_e^2 - 6 |\mathbf{p}_1| |\mathbf{p}_2| x_1 x_2 \right) \\
&+ 2 \left(2 E_1^3 E_2^3 + 2 k \cdot p_1 m_e^4 - (k \cdot p_1)^2 m_e^4 - k \cdot p_2^2 m_e^4 - m_e^6 \right. \\
&- 2 k \cdot p_1 \left(k \cdot p_2 + m_e^2 \right) |\mathbf{p}_1| |\mathbf{p}_2| x_1 x_2 + 2 m_e^4 |\mathbf{p}_1| |\mathbf{p}_2| x_1 x_2 \\
&+ E_1^2 E_2^2 \left(-2 k \cdot p_2 + m_e^2 - 6 |\mathbf{p}_1| |\mathbf{p}_2| x_1 x_2 \right) \\
&+ |\mathbf{p}_1| |\mathbf{p}_2| x_1 x_2 \left(|\mathbf{p}_1| |\mathbf{p}_2| x_1 x_2 \left(m_e^2 - 2 |\mathbf{p}_1| |\mathbf{p}_2| x_1 x_2 \right) \right. \\
&+ k \cdot p_2 \left(2 m_e^2 - 2 |\mathbf{p}_1| |\mathbf{p}_2| x_1 x_2 \right) \\
&+ 2 E_1 E_2 \left(k \cdot p_1 \left(k \cdot p_2 + m_e^2 \right) - m_e^4 + k \cdot p_2 \left(-m_e^2 + 2 |\mathbf{p}_1| |\mathbf{p}_2| x_1 x_2 \right) \right. \\
&+ \left. \left. \left. |\mathbf{p}_1| |\mathbf{p}_2| x_1 x_2 \left(-m_e^2 + 3 |\mathbf{p}_1| |\mathbf{p}_2| x_1 x_2 \right) \right) \right) \right) \left. \right\} \tag{A.2}
\end{aligned}$$

2. $d_2 \neq 0$, $\left|\frac{d_1}{d_2}\right| \geq 1$;

$$\begin{aligned}
I_{F_1} &= \frac{256\pi}{m_e^2 - k \cdot p_1} \left\{ C_V'^2 \left[-3m_e^4 + 2E_1^2 E_2^2 + 2(k \cdot p_1)^2 - 4m_e^2 k \cdot p_2 \right. \right. \\
&+ E_1 E_2 \left(3m_e^2 + 2k \cdot p_1 - 4|\mathbf{p}_1| |\mathbf{p}_2| x_1 x_2 \right) \\
&+ k \cdot p_1 \left(4m_e^2 + 4k \cdot p_2 - 2|\mathbf{p}_1| |\mathbf{p}_2| x_1 x_2 \right) \\
&+ |\mathbf{p}_1| |\mathbf{p}_2| \left(-3m_e^2 x_1 x_2 + |\mathbf{p}_1| |\mathbf{p}_2| \left(1 - x_1^2 + (-1 + 3x_1^2) x_2^2 \right) \right) \left. \right] \\
&+ C_A'^2 \left[-m_e^4 + 2E_1^2 E_2^2 + 2(k \cdot p_1)^2 - 3m_e^2 k \cdot p_2 \right. \\
&+ E_1 E_2 \left(-m_e^2 + 2k \cdot p_1 - 4|\mathbf{p}_1| |\mathbf{p}_2| x_1 x_2 \right) \\
&+ k \cdot p_1 \left(-m_e^2 + 4k \cdot p_2 - 2|\mathbf{p}_1| |\mathbf{p}_2| x_1 x_2 \right) \\
&+ |\mathbf{p}_1| |\mathbf{p}_2| \left(m_e^2 x_1 x_2 + |\mathbf{p}_1| |\mathbf{p}_2| \left(1 - x_1^2 + (-1 + 3x_1^2) x_2^2 \right) \right) \left. \right] \\
&- 2 \frac{(k \cdot p_1 - m_e^2) k \cdot (p_1 + p_2)}{\sqrt{\frac{pole-1}{pole+1}}} \\
&\times \left[-m_e^2 - E_1 E_2 + k \cdot (p_1 + p_2) + |\mathbf{p}_1| |\mathbf{p}_2| x_1 x_2 - |\mathbf{p}_1| |\mathbf{p}_2| \sqrt{1 - x_1^2} \sqrt{1 - x_2^2} \right]^{-1} \\
&\times \left[C_A'^2 \left(-m_e^2 + k \cdot (p_1 + 2p_2) \right) + C_V'^2 \left(2m_e^2 + k \cdot (p_1 + 2p_2) \right) \right] \quad (A.3)
\end{aligned}$$

where

$$pole = \frac{m_e^2 + E_1 E_2 - k \cdot (p_1 + p_2) - |\mathbf{p}_1| |\mathbf{p}_2| x_1 x_2}{|\mathbf{p}_1| |\mathbf{p}_2| \sqrt{(1 - x_1^2)(1 - x_2^2)}}, \quad (A.4)$$

3. $d_2 \neq 0$, $\left|\frac{d_1}{d_2}\right| < 1$;

$$\begin{aligned}
I_{F_1} &= \frac{256\pi}{m_e^2 - k \cdot p_1} \left\{ C_V'^2 \left[2E_1^2 E_2^2 + 2(k \cdot p_1)^2 - 4m_e^2 k \cdot p_2 - 3m_e^4 \right. \right. \\
&+ E_1 E_2 \left(2k \cdot p_1 + 3m_e^2 - 4|\mathbf{p}_1| |\mathbf{p}_2| x_1 x_2 \right) \\
&+ k \cdot p_1 \left(4k \cdot p_2 + 4m_e^2 - 2|\mathbf{p}_1| |\mathbf{p}_2| x_1 x_2 \right) \\
&+ |\mathbf{p}_1| |\mathbf{p}_2| \left(-3m_e^2 x_1 x_2 + |\mathbf{p}_1| |\mathbf{p}_2| \left(1 - x_1^2 + (-1 + 3x_1^2) x_2^2 \right) \right) \left. \right] \\
&+ C_A'^2 \left[2E_1^2 E_2^2 + 2(k \cdot p_1)^2 - 3k \cdot p_2 m_e^2 - m_e^4 \right. \\
&+ E_1 E_2 \left(2k \cdot p_1 - m_e^2 - 4|\mathbf{p}_1| |\mathbf{p}_2| x_1 x_2 \right) \\
&+ k \cdot p_1 \left(4k \cdot p_2 - m_e^2 - 2|\mathbf{p}_1| |\mathbf{p}_2| x_1 x_2 \right) \\
&+ |\mathbf{p}_1| |\mathbf{p}_2| \left(m_e^2 x_1 x_2 + |\mathbf{p}_1| |\mathbf{p}_2| \left(1 - x_1^2 + (-1 + 3x_1^2) x_2^2 \right) \right) \left. \right] \quad (A.5)
\end{aligned}$$

The functions I_{F_2} in the same three cases above are obtained from the previous ones with the substitutions $k \rightarrow -k$ and $p_1 \leftrightarrow p_2$.

B Bremsstrahlung functions

The functions entering in Eq.(3.65) are the following:

$$\begin{aligned}
\Phi_1^E &= 512 \left\{ C_V'^2 \left[(k \cdot p_1)^2 \left(p_1 \cdot p_2 - 2 \left(m_e^2 + k \cdot p_2 \right) \right) \right. \right. \\
&\quad - 2 m_e^2 \left(m_e^2 - k \cdot p_2 + p_1 \cdot p_2 \right) \left(2 m_e^2 - k \cdot p_2 + p_1 \cdot p_2 \right) \\
&\quad + 2 k \cdot p_1 \left(4 m_e^4 - (k \cdot p_2)^2 + 3 m_e^2 p_1 \cdot p_2 + k \cdot p_2 \left(p_1 \cdot p_2 - 2 m_e^2 \right) \right) \\
&\quad + C_A'^2 \left[2 m_e^6 - 2 m_e^2 \left((k - p_2) \cdot p_1 \right)^2 + (k \cdot p_1)^2 \left(4 m_e^2 - 2 k \cdot p_2 + p_1 \cdot p_2 \right) \right. \\
&\quad \left. \left. - 2 k \cdot p_1 \left(2 m_e^4 + (k \cdot p_2)^2 - k \cdot p_2 \left(m_e^2 + p_1 \cdot p_2 \right) \right) \right] \right\} , \tag{B.1}
\end{aligned}$$

$$\begin{aligned}
\Phi_2^E &= 512 \left\{ C_V'^2 \left[-2 \left(2 m_e^6 - 4 m_e^4 k \cdot p_2 + (k \cdot p_1)^2 \left(m_e^2 + k \cdot p_2 \right) + m_e^2 (k \cdot p_2)^2 \right) \right. \right. \\
&\quad + 2 k \cdot p_1 \left(3 m_e^4 - \left(2 m_e^2 + k \cdot p_2 \right) \left(k \cdot p_2 - p_1 \cdot p_2 \right) \right) \\
&\quad - \left(6 m_e^4 - 6 m_e^2 k \cdot p_2 - (k \cdot p_2)^2 \right) p_1 \cdot p_2 - 2 m_e^2 (p_1 \cdot p_2)^2 \\
&\quad + C_A'^2 \left[2 m_e^6 - 2 (k \cdot p_1)^2 \left(m_e^2 + k \cdot p_2 \right) - 2 k \cdot p_2 \left(2 m_e^4 + k \cdot p_1 \left(k \cdot p_2 - m_e^2 \right) \right) \right. \\
&\quad + 4 m_e^2 (k \cdot p_2)^2 + \left(2 k \cdot p_1 \left(2 m_e^2 + k \cdot p_2 \right) + (k \cdot p_2)^2 \right) p_1 \cdot p_2 \\
&\quad \left. \left. - 2 m_e^2 (p_1 \cdot p_2)^2 \right] \right\} , \tag{B.2}
\end{aligned}$$

$$\begin{aligned}
\Phi_{12}^E &= 512 \left\{ C_V'^2 \left[2 m_e^4 k \cdot p_2 - m_e^2 (k \cdot p_2)^2 - (k \cdot p_1)^2 \left(m_e^2 - 2 p_1 \cdot p_2 \right) \right. \right. \\
&\quad - 2 m_e^4 p_1 \cdot p_2 + 2 m_e^2 k \cdot p_2 p_1 \cdot p_2 + 2 (k \cdot p_2)^2 p_1 \cdot p_2 \\
&\quad + k \cdot p_1 \left(k \cdot p_2 \left(3 p_1 \cdot p_2 - 4 m_e^2 \right) + 2 \left(m_e^4 + m_e^2 p_1 \cdot p_2 - 2 (p_1 \cdot p_2)^2 \right) \right) \\
&\quad - 4 k \cdot p_2 (p_1 \cdot p_2)^2 + 2 (p_1 \cdot p_2)^3 \\
&\quad + C_A'^2 \left[-m_e^4 k \cdot p_2 + m_e^2 (k \cdot p_2)^2 + 4 m_e^4 p_1 \cdot p_2 - 7 m_e^2 k \cdot p_2 p_1 \cdot p_2 \right. \\
&\quad + 2 (k \cdot p_2)^2 p_1 \cdot p_2 + (k \cdot p_1)^2 \left(m_e^2 + 2 p_1 \cdot p_2 \right) + 2 \left(3 m_e^2 - 2 k \cdot p_2 \right) (p_1 \cdot p_2)^2 \\
&\quad \left. \left. - k \cdot p_1 \left(m_e^4 + \left(7 m_e^2 - 3 k \cdot p_2 \right) p_1 \cdot p_2 + 4 (p_1 \cdot p_2)^2 \right) + 2 (p_1 \cdot p_2)^3 \right] \right\} . \tag{B.3}
\end{aligned}$$

The corresponding functions appearing in Eq.(3.66) are, instead, obtained from the above reported ones by replacing the 4-momentum k with $-k$.

After integration over the angle ϕ as described in Section 3.2.3, the functions I_a for the photon absorption and I_{e0}, I_e for the photon emission, appearing in Eq.(3.72), are the following ($E_{\nu\bar{\nu}}^\pm = E_1 + E_2 \pm |\mathbf{k}|$, $x_{1,2} = \cos \theta_{1,2}$, $s_{1,2} = \sin \theta_{1,2}$, $\epsilon^2 = E_1 E_2 - |\mathbf{p}_1| |\mathbf{p}_2| x_1 x_2$,

$$\mu_{1,2} = E_{1,2} - |\mathbf{p}_{1,2}|x_{1,2})$$

$$\begin{aligned}
I_a &= \frac{128 \pi |\mathbf{k}|}{\mu_1^2 \mu_2^2} \left\{ 3 C_A'^2 E_{\nu\bar{\nu}}^+ \epsilon^2 \mu_1 \mu_2^3 \right. \\
&- C_V'^2 \left[3 m_e^4 \mu_2^3 + m_e^2 \mu_1^3 (3 m_e^2 + E_{\nu\bar{\nu}}^+ \mu_2) + m_e^2 \mu_1^2 \mu_2 (3 m_e^2 - 6 \epsilon^2 + 2 E_{\nu\bar{\nu}}^+ \mu_2) \right. \\
&+ \left. \mu_1 \mu_2^2 (3 m_e^4 + m_e^2 E_{\nu\bar{\nu}}^+ \mu_2 - 3 \epsilon^2 (2 m_e^2 + E_{\nu\bar{\nu}}^+ \mu_2)) \right] \\
&+ (C_A'^2 + C_V'^2) \left[4 \epsilon^4 \mu_1 \mu_2 (\mu_1 + \mu_2) \right. \\
&+ \left. E_{\nu\bar{\nu}}^+ (-m_e^2 \mu_1^4 + |\mathbf{k}| \mu_1 \mu_2 (\mu_1^3 + \mu_1^2 \mu_2 + \mu_1 \mu_2^2) + \mu_2^4 (|\mathbf{k}| \mu_1 - m_e^2)) \right] \\
&+ \left. \epsilon^2 (-2 m_e^2 \mu_1 \mu_2^2 - 2 m_e^2 \mu_2^3 + 2 \mu_1^2 \mu_2 (2 E_{\nu\bar{\nu}}^+ \mu_2 - m_e^2) + \mu_1^3 (3 E_{\nu\bar{\nu}}^+ \mu_2 - 2 m_e^2)) \right. \\
&+ \left. 2 |\mathbf{p}_1|^2 |\mathbf{p}_2|^2 \mu_1 \mu_2 (\mu_1 + \mu_2) (1 - x_1^2) (1 - x_2^2) \right\} , \tag{B.4}
\end{aligned}$$

and

$$I_{e(e0)} = \frac{-64 \pi |\mathbf{k}|}{\mu_1^2 \mu_2^2} (2 \eta_1 + \eta_3) , \quad (a_1 = 0, a_2 \geq 0 \text{ or } a_1 \neq 0, a_2/a_1 \geq 1) \tag{B.5}$$

$$\begin{aligned}
I_{e(e0)} &= \frac{-64 |\mathbf{k}|}{\mu_1^2 \mu_2^2} \left[2 (\pi - \alpha) \eta_1 - 2 \sin \alpha \eta_2 + (\pi - \alpha - \cos \alpha \sin \alpha) \eta_3 \right. \\
&- \left. \frac{9 \sin \alpha + \sin 3 \alpha}{6} \eta_4 \right] , \quad (a_1 \neq 0, -1 < a_2/a_1 < 1) \tag{B.6}
\end{aligned}$$

where a_1 , a_2 , and α have been defined in Section 3.2.3 and we have introduced the following functions ($\zeta = 0$ for I_e while $\zeta = 1$ for I_{e0}):

$$\begin{aligned}
\eta_1 &= C_V'^2 \left[3 m_e^4 (\mu_1 + \mu_2) (\mu_1^2 + \mu_2^2) \right. \\
&+ (\mu_1 + \mu_2) \left(-4 E_1^2 E_2^2 \mu_1 \mu_2 + E_{\nu\bar{\nu}}^- |\mathbf{k}| \mu_1 \mu_2 (\mu_1^2 + \mu_2^2) \right) \\
&+ \left. m_e^2 \left(2 \epsilon^2 (\mu_1 + \mu_2) (\mu_1^2 - 3 \mu_1 \mu_2 + \mu_2^2) + E_{\nu\bar{\nu}}^- (\mu_1^2 + \mu_2^2) (\mu_1^2 + \mu_1 \mu_2 + \mu_2^2) \right) \right] \\
&+ C_A'^2 \left[\mu_1 \mu_2 (\mu_1 + \mu_2) \left(-4 E_1^2 E_2^2 + E_{\nu\bar{\nu}}^- |\mathbf{k}| (\mu_1^2 + \mu_2^2) \right) \right. \\
&+ \left. m_e^2 \left(2 \epsilon^2 (\mu_1 + \mu_2) (\mu_1^2 + \mu_2^2) + E_{\nu\bar{\nu}}^- (\mu_1^4 + \mu_2^4) \right) \right] \\
&+ (C_A'^2 + C_V'^2) \mu_1 \mu_2 \left[-E_{\nu\bar{\nu}}^- \epsilon^2 (3 \mu_1^2 + 4 \mu_1 \mu_2 + 3 \mu_2^2) \right. \\
&+ \left. 4 (E_1 E_2 + \epsilon^2) (\mu_1 + \mu_2) |\mathbf{p}_1| |\mathbf{p}_2| x_1 x_2 \right] \\
&+ \zeta \frac{2 \epsilon^2 \mu_1 \mu_2 - m_e^2 (\mu_1^2 + \mu_2^2)}{|\mathbf{k}|^2} \left\{ C_V'^2 \left[-E_{\nu\bar{\nu}}^- (\epsilon^4 + 3 m_e^2 \epsilon^2 + 2 m_e^4) \right. \right. \\
&+ \left. \left. 3 m_e^2 |\mathbf{k}| (E_1 + E_2) (\mu_1 + \mu_2) \right] \right. \\
&+ \left. C_A'^2 \left[-E_{\nu\bar{\nu}}^- (E_1^2 E_2^2 - m_e^4) + E_{\nu\bar{\nu}}^- (E_1 E_2 + \epsilon^2) |\mathbf{p}_1| |\mathbf{p}_2| x_1 x_2 \right] \right. \\
&+ \left. 2 (C_A'^2 + C_V'^2) \epsilon^2 |\mathbf{k}| (E_1 + E_2) (\mu_1 + \mu_2) \right\} , \tag{B.7}
\end{aligned}$$

$$\begin{aligned}
\eta_2 = & |\mathbf{p}_1| |\mathbf{p}_2| s_1 s_2 \left\{ 6 C_V'^2 m_e^2 \mu_1 \mu_2 (\mu_1 + \mu_2) \right. \\
& + \left(C_A'^2 + C_V'^2 \right) \left[-2 m_e^2 (\mu_1 + \mu_2) (\mu_1^2 + \mu_2^2) + \mu_1 \mu_2 \left(8 \epsilon^2 (\mu_1 + \mu_2) \right. \right. \\
& + \left. \left. E_{\nu\bar{\nu}}^- (3 \mu_1^2 + 4 \mu_1 \mu_2 + 3 \mu_2^2) \right) \right] \left. \right\} \\
& + \zeta \frac{|\mathbf{p}_1| |\mathbf{p}_2| s_1 s_2}{|\mathbf{k}|^2} \left\{ -2 C_A'^2 m_e^4 E_{\nu\bar{\nu}}^- \mu_1 \mu_2 \right. \\
& + C_V'^2 \left[-6 m_e^2 (E_1 + E_2) |\mathbf{k}| \mu_1 \mu_2 (\mu_1 + \mu_2) + E_{\nu\bar{\nu}}^- \left(12 m_e^2 \epsilon^2 \mu_1 \mu_2 \right. \right. \\
& + \left. \left. m_e^4 (-3 \mu_1^2 + 4 \mu_1 \mu_2 - 3 \mu_2^2) \right) \right] \\
& + \left(C_A'^2 + C_V'^2 \right) \left[2 E_{\nu\bar{\nu}}^- \epsilon^2 \left(3 \epsilon^2 \mu_1 \mu_2 - m_e^2 (\mu_1^2 + \mu_2^2) \right) \right. \\
& + \left. \left. 2 (E_1 + E_2) |\mathbf{k}| (\mu_1 + \mu_2) \left(-4 \epsilon^2 \mu_1 \mu_2 + m_e^2 (\mu_1^2 + \mu_2^2) \right) \right) \right] \left. \right\} , \tag{B.8}
\end{aligned}$$

$$\begin{aligned}
\eta_3 = & -4 \left(C_A'^2 + C_V'^2 \right) |\mathbf{p}_1|^2 |\mathbf{p}_2|^2 \mu_1 \mu_2 (\mu_1 + \mu_2) s_1^2 s_2^2 \\
& + \zeta \frac{|\mathbf{p}_1|^2 |\mathbf{p}_2|^2 s_1^2 s_2^2}{|\mathbf{k}|^2} \left\{ -6 C_V'^2 m_e^2 E_{\nu\bar{\nu}}^- \mu_1 \mu_2 \right. \\
& + \left(C_A'^2 + C_V'^2 \right) \left[-6 E_{\nu\bar{\nu}}^- \epsilon^2 \mu_1 \mu_2 + 4 (E_1 + E_2) |\mathbf{k}| \mu_1 \mu_2 (\mu_1 + \mu_2) \right. \\
& + \left. \left. m_e^2 E_{\nu\bar{\nu}}^- (\mu_1^2 + \mu_2^2) \right) \right] \left. \right\} , \tag{B.9}
\end{aligned}$$

$$\eta_4 = \zeta \frac{2 \left(C_A'^2 + C_V'^2 \right) E_{\nu\bar{\nu}}^- |\mathbf{p}_1|^3 |\mathbf{p}_2|^3 \mu_1 \mu_2 s_1^3 s_2^3}{|\mathbf{k}|^2} . \tag{B.10}$$

C Photoproduction functions

The functions entering in Eq.(4.77) are given by

$$\begin{aligned}
\Phi_{ph}^1 = & C_V'^2 \left\{ -32 (k \cdot p_1)^3 m_e^2 + 4 k \cdot p_1 (8 m_e^4 m_\gamma^2 + 3 m_e^2 m_\gamma^4) \right. \\
& + 4 (k \cdot p_1)^2 \left[-8 m_e^4 + k \cdot p_2 (8 m_e^2 + 6 m_\gamma^2) + 7 m_\gamma^2 p_1 \cdot p_2 \right. \\
& + \left. \left. m_e^2 (-7 m_\gamma^2 + 12 p_1 \cdot p_2) \right] + m_\gamma^2 \left[32 m_e^6 - 16 k \cdot p_2 (3 m_e^4 + 2 m_e^2 m_\gamma^2) \right. \right. \\
& + \left. \left. 8 m_e^4 (5 m_\gamma^2 - 6 p_1 \cdot p_2) - m_\gamma^4 p_1 \cdot p_2 + 9 m_e^2 (m_\gamma^4 - 4 m_\gamma^2 p_1 \cdot p_2) \right] \right\} \\
& + C_A'^2 \left\{ 16 (k \cdot p_1)^3 m_e^2 - 8 k \cdot p_1 (2 m_e^4 m_\gamma^2 + 3 m_e^2 m_\gamma^4) \right. \\
& - 4 (k \cdot p_1)^2 \left(4 k \cdot p_2 m_e^2 - 4 m_e^4 - 6 k \cdot p_2 m_\gamma^2 + m_e^2 m_\gamma^2 - 7 m_\gamma^2 p_1 \cdot p_2 \right) \\
& - \left. \left. m_\gamma^2 \left[m_e^2 \left(16 m_e^4 - 4 (k \cdot p_2 - 5 m_e^2) m_\gamma^2 + 9 m_\gamma^4 \right) + m_\gamma^4 p_1 \cdot p_2 \right] \right\} \right. \\
& + 2 \left(C_A'^2 + C_V'^2 \right) \left\{ -8 (k \cdot p_1)^2 p_1 \cdot p_2 (k \cdot p_2 + p_1 \cdot p_2) \right. \\
& + 4 (k \cdot p_1)^3 (k \cdot p_2 + 2 p_1 \cdot p_2) + 2 m_\gamma^2 (k \cdot p_2 + p_1 \cdot p_2) \left(4 k \cdot p_2 m_e^2 \right. \\
& + \left. \left. (4 m_e^2 + m_\gamma^2) p_1 \cdot p_2 \right) + k \cdot p_1 m_\gamma^2 \left(-8 (k \cdot p_2)^2 \right. \right.
\end{aligned}$$

$$+ k \cdot p_2 (5 m_\gamma^2 - 16 p_1 \cdot p_2) + 4 (m_\gamma^2 - 2 p_1 \cdot p_2) p_1 \cdot p_2 \} , \quad (\text{C.11})$$

$$\begin{aligned} \Phi_{ph}^2 &= C_V'^2 \left\{ -8 k \cdot p_1 \left[4 (k \cdot p_2)^2 m_e^2 + 3 \left((k \cdot p_2)^2 - 2 m_e^4 \right) m_\gamma^2 - 4 m_e^2 m_\gamma^4 \right] \right. \\ &+ m_e^2 \left[32 (k \cdot p_2)^2 (k \cdot p_2 - m_e^2) - 4 \left(7 (k \cdot p_2)^2 + 8 k \cdot p_2 m_e^2 - 8 m_e^4 \right) m_\gamma^2 \right. \\ &- 4 (3 k \cdot p_2 - 10 m_e^2) m_\gamma^4 + 9 m_\gamma^6 \left. \right] - \left[48 m_e^4 m_\gamma^2 + 36 m_e^2 m_\gamma^4 + m_\gamma^6 \right. \\ &- 4 (k \cdot p_2)^2 (12 m_e^2 + 7 m_\gamma^2) \left. \right] p_1 \cdot p_2 \left. \right\} \\ &+ C_A'^2 \left\{ m_e^2 \left[-16 (k \cdot p_2)^2 (k \cdot p_2 - m_e^2) - 4 (k \cdot p_2 - 2 m_e^2)^2 m_\gamma^2 \right. \right. \\ &+ 4 (6 k \cdot p_2 - 5 m_e^2) m_\gamma^4 - 9 m_\gamma^6 \left. \right] - 4 k \cdot p_1 \left(m_e^2 m_\gamma^4 \right. \\ &+ (k \cdot p_2)^2 (-4 m_e^2 + 6 m_\gamma^2) \left. \right) - m_\gamma^2 \left(-28 (k \cdot p_2)^2 + m_\gamma^4 \right) p_1 \cdot p_2 \left. \right\} \\ &+ 2 \left(C_A'^2 + C_V'^2 \right) \left\{ k \cdot p_1 \left[4 (k \cdot p_2)^3 + 8 k \cdot p_1 (k \cdot p_2 + m_e^2) m_\gamma^2 \right. \right. \\ &+ 5 k \cdot p_2 m_\gamma^4 \left. \right] + 2 \left[4 k \cdot (p_1 - p_2) (k \cdot p_2)^2 - 8 k \cdot p_1 (k \cdot p_2 + m_e^2) m_\gamma^2 \right. \\ &- (k \cdot p_1 + 2 k \cdot p_2) m_\gamma^4 \left. \right] p_1 \cdot p_2 - 2 \left[4 (k \cdot p_2)^2 \right. \\ &- 4 (k \cdot p_2 + m_e^2) m_\gamma^2 - m_\gamma^4 \left. \right] (p_1 \cdot p_2)^2 \left. \right\} , \quad (\text{C.12}) \end{aligned}$$

$$\begin{aligned} \Phi_{ph}^{12} &= C_V'^2 \left\{ -4 (k \cdot p_1)^2 \left(8 k \cdot p_2 m_e^2 + (k \cdot p_2 - 2 m_e^2) m_\gamma^2 \right) \right. \\ &+ m_\gamma^2 \left[8 (k \cdot p_2)^2 m_e^2 + 32 m_e^4 p_1 \cdot p_2 + 5 m_\gamma^2 (m_\gamma^2 - 4 p_1 \cdot p_2) p_1 \cdot p_2 \right. \\ &+ m_e^2 \left(3 m_\gamma^4 + 28 m_\gamma^2 p_1 \cdot p_2 - 48 (p_1 \cdot p_2)^2 \right) - 2 k \cdot p_2 \left(4 m_e^4 \right. \\ &+ 7 m_\gamma^2 p_1 \cdot p_2 + m_e^2 (5 m_\gamma^2 + 16 p_1 \cdot p_2) \left. \right) \left. \right] + 2 k \cdot p_1 \left[2 (k \cdot p_2)^2 (8 m_e^2 + m_\gamma^2) \right. \\ &- k \cdot p_2 \left(16 m_e^4 + m_\gamma^4 + m_e^2 (22 m_\gamma^2 - 24 p_1 \cdot p_2) + 2 m_\gamma^2 p_1 \cdot p_2 \right) \\ &+ m_\gamma^2 \left(4 m_e^4 + 7 m_\gamma^2 p_1 \cdot p_2 + m_e^2 (5 m_\gamma^2 + 16 p_1 \cdot p_2) \right) \left. \right] \left. \right\} \\ &+ C_A'^2 \left\{ 4 (k \cdot p_1)^2 k \cdot p_2 (4 m_e^2 - m_\gamma^2) + m_\gamma^2 \left[-3 m_e^2 m_\gamma^4 \right. \right. \\ &+ 4 m_e^4 (m_\gamma^2 - 4 p_1 \cdot p_2) + 5 m_\gamma^2 (m_\gamma^2 - 4 p_1 \cdot p_2) p_1 \cdot p_2 \\ &- 2 k \cdot p_2 \left(4 m_e^4 + 7 m_\gamma^2 p_1 \cdot p_2 - m_e^2 (m_\gamma^2 + 8 p_1 \cdot p_2) \right) \left. \right] \\ &- 2 k \cdot p_1 \left[(k \cdot p_2)^2 (8 m_e^2 - 2 m_\gamma^2) + k \cdot p_2 (-8 m_e^4 + 2 m_e^2 m_\gamma^2 + m_\gamma^4 \right. \\ &+ 2 m_\gamma^2 p_1 \cdot p_2) + m_\gamma^2 \left(-4 m_e^4 - 7 m_\gamma^2 p_1 \cdot p_2 + m_e^2 (m_\gamma^2 + 8 p_1 \cdot p_2) \right) \left. \right] \left. \right\} \\ &+ 8 \left(C_A'^2 + C_V'^2 \right) \left\{ m_\gamma^2 p_1 \cdot p_2 (k \cdot p_2 + p_1 \cdot p_2) (k \cdot p_2 + 2 p_1 \cdot p_2) \right. \\ &+ (k \cdot p_1)^2 \left((k \cdot p_2)^2 + 2 k \cdot p_2 p_1 \cdot p_2 + m_\gamma^2 p_1 \cdot p_2 \right) \\ &- k \cdot p_1 p_1 \cdot p_2 \left(2 (k \cdot p_2)^2 + 2 k \cdot p_2 p_1 \cdot p_2 + 3 m_\gamma^2 p_1 \cdot p_2 \right) \left. \right\} . \quad (\text{C.13}) \end{aligned}$$

The function I_{ph} appearing in Eq.(4.82) is obtained after integration over the angle ϕ . In particular, one has

$$I_{ph} = \frac{128 \pi |\mathbf{k}|^2 (E_1 - E_2 + E_\gamma)}{E_\gamma (m_\gamma^2 + 2 k \cdot p_1)^2 (m_\gamma^2 - 2 k \cdot p_1)^2} (2 \nu_1 + \nu_3) \quad b_1 = 0, \quad b_2 \leq 0, \quad (\text{C.14})$$

$$I_{ph} = \frac{128 |\mathbf{k}|^2 (E_1 - E_2 + E_\gamma)}{E_\gamma (m_\gamma^2 + 2 k \cdot p_1)^2 (m_\gamma^2 - 2 k \cdot p_1)^2} \left[2 \beta \nu_1 + 2 \sin \beta \nu_2 + (\beta + \cos \beta \sin \beta) \nu_3 + \frac{9 \sin \beta + \sin 3\beta}{6} \nu_4 \right] \quad b_1 \neq 0, \quad -1 < b_2/b_1 < 1, \quad (\text{C.15})$$

and the functions ν_i are ($x_{1,2} = \cos \theta_{1,2}$, $s_{1,2} = \sin \theta_{1,2}$, $\epsilon^2 = E_1 E_2 - |\mathbf{p}_1| |\mathbf{p}_2| x_1 x_2$)

$$\begin{aligned} \nu_1 = & C_A'^2 \left\{ -8 k \cdot p_1 k \cdot p_2 \left[2 \epsilon^6 - 4 \epsilon^4 k \cdot (p_1 - p_2) - k \cdot (p_1 - p_2) \left((k \cdot p_1)^2 + (k \cdot p_2)^2 \right) \right] \right. \\ & + \epsilon^2 \left(3 (k \cdot p_1)^2 - 4 k \cdot p_1 k \cdot p_2 + 3 (k \cdot p_2)^2 \right) \\ & + 8 m_e^2 \left[(k \cdot p_1)^4 + \epsilon^2 \left(\epsilon^2 - 2 k \cdot (p_1 - p_2) \right) \left((k \cdot p_1)^2 + (k \cdot p_2)^2 \right) + (k \cdot p_2)^4 \right] \\ & + 16 m_e^4 \epsilon^2 k \cdot p_1 k \cdot p_2 - 8 m_e^6 \left((k \cdot p_1)^2 + (k \cdot p_2)^2 \right) \\ & + 4 m_\gamma^2 \left[-3 \epsilon^4 (k \cdot p_1)^2 + 2 \epsilon^6 k \cdot (p_1 - p_2) + \epsilon^2 k \cdot (p_1 - p_2) \left((k \cdot p_1)^2 + (k \cdot p_2)^2 \right) \right. \\ & + 14 \epsilon^4 k \cdot p_1 k \cdot p_2 - 12 \epsilon^2 k \cdot p_1 k \cdot p_2 k \cdot (p_1 - p_2) \\ & + 3 k \cdot p_1 \left((k \cdot p_1)^2 + (k \cdot p_2)^2 \right) k \cdot p_2 - 3 \epsilon^4 (k \cdot p_2)^2 - 4 (k \cdot p_1)^2 (k \cdot p_2)^2 \\ & + 2 m_e^2 \left((k \cdot p_1)^3 + \epsilon^2 k \cdot (p_1 - p_2) (\epsilon^2 - k \cdot (p_1 - p_2)) \right) \\ & - 2 \epsilon^2 \left((k \cdot p_1)^2 + (k \cdot p_2)^2 \right) + 2 k \cdot p_1 k \cdot (p_1 - p_2) k \cdot p_2 - (k \cdot p_2)^3 \Big] \\ & - m_e^4 k \cdot (p_1 - p_2) \left(2 \epsilon^2 + k \cdot (p_1 - p_2) \right) - 2 m_e^6 k \cdot (p_1 - p_2) \Big] \\ & + 2 m_\gamma^4 \left[2 \epsilon^6 + 5 \epsilon^2 (k \cdot p_1)^2 - 8 \epsilon^4 k \cdot (p_1 - p_2) - 18 \epsilon^2 k \cdot p_1 k \cdot p_2 \right. \\ & + 4 k \cdot p_1 k \cdot p_2 k \cdot (p_1 - p_2) + 5 \epsilon^2 (k \cdot p_2)^2 - 2 m_e^6 + m_e^2 \left(2 \epsilon^2 (\epsilon^2 - 2 k \cdot (p_1 - p_2)) \right. \\ & - 3 \left((k \cdot p_1)^2 + (k \cdot p_2)^2 \right) + 14 k \cdot p_1 k \cdot p_2 \left. \right) - 2 m_e^4 \left(\epsilon^2 + 2 k \cdot (p_1 - p_2) \right) \Big] \\ & - 2 m_\gamma^6 \left[2 \epsilon^4 - 3 \epsilon^2 k \cdot (p_1 - p_2) - k \cdot p_1 k \cdot p_2 + 5 m_e^2 k \cdot (p_1 - p_2) + 2 m_e^4 \right] \\ & + m_\gamma^8 (\epsilon^2 - 3 m_e^2) \Big\} \\ & + C_V'^2 \left[2 m_e^2 + m_\gamma^2 - 2 \epsilon^2 + 2 k \cdot (p_1 - p_2) \right] \\ & \times \left\{ 2 \epsilon^4 \left(2 k \cdot p_2 - m_\gamma^2 \right) \left(2 k \cdot p_1 + m_\gamma^2 \right) + \epsilon^2 \left[-8 k \cdot p_1 k \cdot p_2 k \cdot (p_1 - p_2) \right. \right. \\ & - 4 m_e^2 \left(\left((k \cdot p_1)^2 + (k \cdot p_2)^2 \right) + 4 k \cdot p_1 k \cdot p_2 \right) + 2 m_\gamma^2 \left((k \cdot (p_1 - p_2))^2 \right. \\ & - 6 k \cdot p_1 k \cdot p_2 + 2 m_e^2 k \cdot (p_1 - p_2) \left. \right) + 2 m_\gamma^4 \left(2 k \cdot (p_1 - p_2) + m_e^2 \right) + m_\gamma^6 \Big] \\ & \left. + \left[2 \left((k \cdot p_1)^2 + (k \cdot p_2)^2 \right) + 2 m_\gamma^2 k \cdot (p_1 - p_2) + m_\gamma^4 \right] \left[2 k \cdot p_1 \left(k \cdot p_2 + m_e^2 \right) \right] \right\} \end{aligned}$$

$$+ m_e^2 \left(-2 k \cdot p_2 + 4 m_e^2 + 3 m_\gamma^2 \right) \} , \quad (\text{C.16})$$

$$\begin{aligned} \nu_2 = & |\mathbf{p}_1| |\mathbf{p}_2| s_1 s_2 \left\{ C_A'^2 \left\{ 8 k \cdot p_1 k \cdot p_2 \left[-8 \epsilon^2 k \cdot (p_1 - p_2) + 3 \left((k \cdot p_1)^2 + (k \cdot p_2)^2 \right) \right. \right. \right. \\ & - 4 k \cdot p_1 k \cdot p_2 + 6 \epsilon^4 \left. \left. \left. \right] - 16 m_e^2 \left[-(k \cdot p_1)^3 + \epsilon^2 \left((k \cdot p_1)^2 + (k \cdot p_2)^2 \right) + (k \cdot p_2)^3 \right. \right. \right. \\ & + k \cdot p_1 k \cdot p_2 k \cdot (p_1 - p_2) \left. \left. \left. \right] - 16 m_e^4 k \cdot p_1 k \cdot p_2 + m_\gamma^2 \left[-4 \left(6 \epsilon^4 k \cdot (p_1 - p_2) \right. \right. \right. \\ & - 6 \epsilon^2 \left((k \cdot p_1)^2 + (k \cdot p_2)^2 \right) + k \cdot p_1 k \cdot p_2 \left(28 \epsilon^2 - 13 k \cdot (p_1 - p_2) \right) - (k \cdot p_2)^3 \right. \right. \\ & + (k \cdot p_1)^3 \left. \left. \left. \right] + 8 m_e^2 \left(-2 \epsilon^2 k \cdot (p_1 - p_2) + 3 \left((k \cdot p_1)^2 + (k \cdot p_2)^2 \right) - 2 k \cdot p_1 k \cdot p_2 \right) \right. \right. \\ & + 8 m_e^4 k \cdot (p_1 - p_2) \left. \left. \left. \right] - 2 m_\gamma^4 \left[6 \epsilon^4 - 16 \epsilon^2 k \cdot (p_1 - p_2) + 5 \left((k \cdot p_1)^2 + (k \cdot p_2)^2 \right) \right. \right. \right. \\ & - 18 k \cdot p_1 k \cdot p_2 + 4 m_e^2 \left(\epsilon^2 - k \cdot (p_1 - p_2) \right) + 4 m_e^4 \left. \left. \left. \right] \right. \right. \\ & + 2 m_\gamma^6 \left(4 \epsilon^2 - 3 k \cdot (p_1 - p_2) \right) - m_\gamma^8 \left. \left. \left. \right\} \right. \right. \\ & + C_V'^2 \left\{ 8 k \cdot p_1 k \cdot p_2 \left[6 \epsilon^4 - 8 \epsilon^2 k \cdot (p_1 - p_2) + 3 \left((k \cdot p_1)^2 + (k \cdot p_2)^2 \right) \right. \right. \right. \\ & - 4 k \cdot p_1 k \cdot p_2 \left. \left. \left. \right] - 16 m_e^2 \left[-(k \cdot p_1)^3 - 2 k \cdot p_1 k \cdot (p_1 - p_2) k \cdot p_2 + (k \cdot p_2)^3 \right. \right. \right. \\ & + \epsilon^2 \left(\left((k \cdot p_1)^2 + (k \cdot p_2)^2 \right) + 6 k \cdot p_1 k \cdot p_2 \right) \left. \left. \left. \right] + 8 m_e^4 \left[3 \left((k \cdot p_1)^2 + (k \cdot p_2)^2 \right) \right. \right. \right. \\ & + 4 k \cdot p_1 k \cdot p_2 \left. \left. \left. \right] + m_\gamma^2 \left[-4 \left((k \cdot p_1)^3 + 6 \epsilon^4 k \cdot (p_1 - p_2) - (k \cdot p_2)^3 \right. \right. \right. \\ & - 13 k \cdot p_1 k \cdot p_2 k \cdot (p_1 - p_2) + \epsilon^2 \left(-6 (k \cdot p_1)^2 + 28 k \cdot p_1 k \cdot p_2 - 6 (k \cdot p_2)^2 \right) \left. \left. \left. \right) \right. \right. \\ & + m_e^2 \left(32 \epsilon^2 k \cdot (p_1 - p_2) + 12 \left((k \cdot p_1)^2 + (k \cdot p_2)^2 \right) + 48 k \cdot p_1 k \cdot p_2 \right) \left. \left. \left. \right) \right. \right. \\ & + 8 m_e^4 k \cdot (p_1 - p_2) \left. \left. \left. \right] - 2 m_\gamma^4 \left[6 \epsilon^4 + 5 (k \cdot p_1)^2 - 18 k \cdot p_1 k \cdot p_2 + 5 (k \cdot p_2)^2 \right. \right. \right. \\ & - 2 m_e^4 - 8 \epsilon^2 \left(2 k \cdot (p_1 - p_2) + m_e^2 \right) \left. \left. \left. \right] + 2 m_\gamma^6 \left(4 \epsilon^2 - 3 k \cdot (p_1 - p_2) + m_e^2 \right) \right. \right. \\ & - m_\gamma^8 \left. \left. \left. \right\} \right. , \quad (\text{C.17}) \end{aligned}$$

$$\begin{aligned} \nu_3 = & 4 |\mathbf{p}_1|^2 |\mathbf{p}_2|^2 s_1^2 s_2^2 \left\{ \left(C_A'^2 - 2 C_V'^2 \right) m_e^2 m_\gamma^2 \left(2 k \cdot (p_1 - p_2) + m_\gamma^2 \right) \right. \\ & + 12 C_V'^2 m_e^2 k \cdot p_1 k \cdot p_2 - \left(C_A'^2 + C_V'^2 \right) \left\{ 4 k \cdot p_1 k \cdot p_2 \left(3 \epsilon^2 - 2 k \cdot (p_1 - p_2) \right) \right. \\ & - 2 m_e^2 \left((k \cdot p_1)^2 + (k \cdot p_2)^2 \right) + m_\gamma^2 \left[-6 \epsilon^2 k \cdot (p_1 - p_2) + 3 \left((k \cdot p_1)^2 + (k \cdot p_2)^2 \right) \right. \\ & - 14 k \cdot p_1 k \cdot p_2 \left. \left. \left. \right] - m_\gamma^4 \left(3 \epsilon^2 - 4 k \cdot (p_1 - p_2) \right) + m_\gamma^6 \left. \left. \left. \right\} \right. , \quad (\text{C.18}) \end{aligned}$$

$$\nu_4 = 4 \left(C_A'^2 + C_V'^2 \right) |\mathbf{p}_1|^3 |\mathbf{p}_2|^3 s_1^3 s_2^3 \left(2 k \cdot p_2 - m_\gamma^2 \right) \left(2 k \cdot p_1 + m_\gamma^2 \right) \quad (\text{C.19})$$

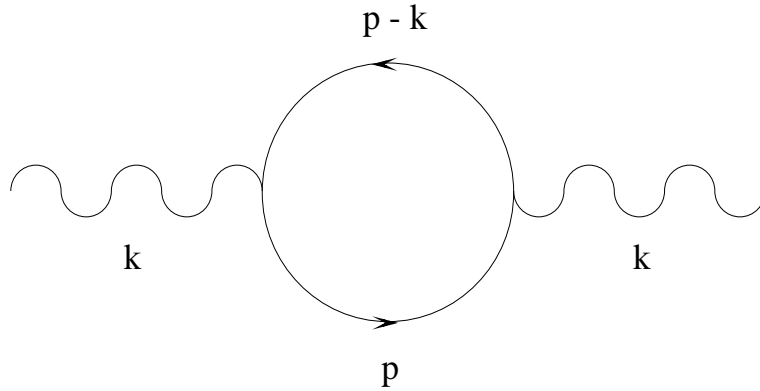


Figure 8: Self-energy diagram for a photon in a plasma.

D Electromagnetic excitations in a plasma

The equation of motion for the 4-vector potential field A^μ of a photon in a plasma can be written as

$$\left(-k^2 g_{\mu\nu} + \Pi_{\mu\nu}\right) A^\nu = 0 \quad , \quad (\text{D.1})$$

where $\Pi_{\mu\nu}$ is the polarization tensor obtained from the diagram in Figure 8 (in the Feynman gauge) [19], [21]:

$$\Pi_{\mu\nu} = -16\pi\alpha \int \frac{d^3\mathbf{p}}{(2\pi)^3} \frac{[F_-(E) + F_+(E)]}{2E} \frac{p \cdot K (K_\mu p_\nu + K_\nu p_\mu) - K^2 p_\mu p_\nu - (p \cdot K)^2 g_{\mu\nu}}{(p \cdot K)^2 - K^4/4} \quad , \quad (\text{D.2})$$

with $p = (E, \mathbf{p})$, $K = (E_\gamma, \mathbf{k})$ and $E_\gamma = \sqrt{|\mathbf{k}|^2 + m_\gamma^2}$, $E = \sqrt{|\mathbf{p}|^2 + m_e^2}$. It is useful to express $\Pi_{\mu\nu}$ in terms of form factors by using Lorentz and gauge invariance, namely $k^\mu \Pi_{\mu\nu} = k^\nu \Pi_{\mu\nu} = 0$. The most general form of $\Pi_{\mu\nu}$ (assuming parity conservation) results to be [28]

$$\Pi_{\mu\nu} = \Pi_T R_{\mu\nu} + \Pi_L Q_{\mu\nu} \quad , \quad (\text{D.3})$$

where $R_{\mu\nu}$ and $Q_{\mu\nu}$ are given in Eqs.(5.95), (5.94). The quantities Π_T and Π_L may be computed from the relations $\Pi_L = Q^{\mu\nu} \Pi_{\mu\nu}$, $\Pi_T = R^{\mu\nu} \Pi_{\mu\nu}$ and the results are ⁴:

$$\begin{aligned} \Pi_T &= \frac{4\alpha}{\pi} \int_0^\infty d|\mathbf{p}| \frac{|\mathbf{p}|^2}{E} \left(\frac{E_\gamma^2}{|\mathbf{k}|^2} - \frac{E_\gamma^2 - |\mathbf{k}|^2}{|\mathbf{k}|^2} \frac{E_\gamma}{2v|\mathbf{k}|} \log \left(\frac{E_\gamma + v|\mathbf{k}|}{E_\gamma - v|\mathbf{k}|} \right) \right) \\ &\times [F_-(E) + F_+(E)] \quad , \end{aligned} \quad (\text{D.4})$$

⁴The expressions in Eqs.(D.4) and (D.5) are obtained by neglecting the term $K^4/4$ in the denominator of Eq.(D.2). As shown in Ref. [19], this introduces only an error of higher order in α and, moreover, eliminate the effects of the unphysical process $\gamma \rightarrow e^+e^-$, since $\Pi_{T,L}$ remain real-valued at all temperatures and densities as they should be.

$$\begin{aligned} \Pi_L &= \frac{4\alpha}{\pi} \frac{E_\gamma^2 - |\mathbf{k}|^2}{|\mathbf{k}|^2} \int_0^\infty d|\mathbf{p}| \frac{|\mathbf{p}|^2}{E} \left(\frac{E_\gamma}{v|\mathbf{k}|} \log \left(\frac{E_\gamma + v|\mathbf{k}|}{E_\gamma - v|\mathbf{k}|} \right) - 1 - \frac{E_\gamma^2 - |\mathbf{k}|^2}{E_\gamma^2 - v^2|\mathbf{k}|^2} \right) \\ &\times [F_-(E) + F_+(E)] \ , \end{aligned} \quad (\text{D.5})$$

where $v = |\mathbf{p}|/E$ is the electron or positron velocity. The integrals in Eqs.(D.4), (D.5) over the electron momentum $|\mathbf{p}|$ are well approximated [19, 21] by the following expressions that we use in our computations for the neutrino energy loss rates

$$\Pi_T = \omega_P^2 \left[1 + \frac{1}{2} G \left(\frac{v_*^2 |\mathbf{k}|^2}{\omega^2} \right) \right] \ , \quad (\text{D.6})$$

$$\Pi_L = \omega_P^2 \left[1 - G \left(\frac{v_*^2 |\mathbf{k}|^2}{\omega^2} \right) \right] + v_*^2 |\mathbf{k}|^2 - |\mathbf{k}|^2 \ , \quad (\text{D.7})$$

where $v_* \equiv \omega_1/\omega_P$, with the definitions

$$\omega_P^2 \equiv \frac{4\alpha}{\pi} \int_0^\infty d|\mathbf{p}| \left(v - \frac{1}{3} v^3 \right) |\mathbf{p}| [F_-(E) + F_+(E)] \ , \quad (\text{D.8})$$

$$\omega_1^2 \equiv \frac{4\alpha}{\pi} \int_0^\infty d|\mathbf{p}| \left(\frac{5}{3} v^3 - v^5 \right) |\mathbf{p}| [F_-(E) + F_+(E)] \ , \quad (\text{D.9})$$

can be interpreted as a typical velocity of the electrons in the medium. The function G is defined by

$$G(x) \equiv \frac{3}{x} \left[1 - \frac{2x}{3} - \frac{1-x}{2\sqrt{x}} \log \left(\frac{1+\sqrt{x}}{1-\sqrt{x}} \right) \right] \ . \quad (\text{D.10})$$

The dispersion relations $E_{\gamma T,L}(|\mathbf{k}|)$ for transverse and longitudinal photon modes are given by the locations of the poles in the effective photon propagator which, in the Feynman gauge, takes the form [28]

$$D_{\mu\nu} = - \frac{R_{\mu\nu}}{K^2 - \Pi_T} - \frac{Q_{\mu\nu}}{K^2 - \Pi_L} \ . \quad (\text{D.11})$$

The explicit expressions for $E_{\gamma T,L}(|\mathbf{k}|)$ are then obtained as the solutions of the implicit equations

$$E_{\gamma T,L}^2 - |\mathbf{k}|^2 = \Pi_{T,L}(E_{\gamma T,L}, |\mathbf{k}|) \ , \quad (\text{D.12})$$

while, near the poles, the scalar parts of the effective propagators are:

$$\frac{1}{K^2 - \Pi_{T,L}} \simeq \frac{Z_{T,L}}{2E_{\gamma T,L}} \frac{1}{E_\gamma - E_{\gamma T,L}} \ , \quad (\text{D.13})$$

with

$$Z_{T,L} = 1 + \frac{1}{2E_{\gamma T,L}} \left. \frac{\partial \Pi_{T,L}}{\partial E_\gamma} \right|_{E_\gamma = E_{\gamma T,L}} \ . \quad (\text{D.14})$$

By inserting Eqs.(D.6), (D.7) into the above equation for $Z_{T,L}$, we obtain the final expressions for the residue functions used in the plasmon decay rate [19], [21]

$$Z_T = \frac{2 E_{\gamma T}^2 (E_{\gamma T}^2 - v_*^2 |\mathbf{k}|^2)}{E_{\gamma T}^2 (3 \omega_P^2 - 2 \Pi_T) + (E_{\gamma T}^2 + |\mathbf{k}|^2)(E_{\gamma T}^2 - v_*^2 |\mathbf{k}|^2)} , \quad (\text{D.15})$$

$$Z_L = \frac{2 E_{\gamma L}^2 (E_{\gamma L}^2 - v_*^2 |\mathbf{k}|^2)}{[3 \omega_P^2 - (E_{\gamma L}^2 - v_*^2 |\mathbf{k}|^2)] \Pi_L} . \quad (\text{D.16})$$

From Eq.(D.12) we can see that $E_{\gamma T} > |\mathbf{k}|$ for all $|\mathbf{k}|$ while $E_{\gamma L} > |\mathbf{k}|$ only for $|\mathbf{k}| < |\mathbf{k}|_{max}$ with [19]

$$|\mathbf{k}|_{max}^2 = \frac{4\alpha}{\pi} \int_0^\infty d|\mathbf{p}| \frac{|\mathbf{p}|^2}{E} \left(\frac{1}{v} \log \left(\frac{1+v}{1-v} \right) - 1 \right) [F_-(E) + F_+(E)] . \quad (\text{D.17})$$

Then longitudinal photon modes can decay into neutrino pairs if their momentum is lower than the maximum value $|\mathbf{k}|_{max}$. Note that to the same level of approximation as for Eqs.(D.6), (D.7) we have [19]

$$|\mathbf{k}|_{max} = \omega_P \left[\frac{3}{v_*^2} \left(\frac{1}{2v_*} \log \left(\frac{1+v_*}{1-v_*} \right) - 1 \right) \right]^{1/2} . \quad (\text{D.18})$$

References

- [1] see for example H.T. Janka, K. Kifonidis, and M. Rampp, Proc. of *ECT International Workshop on Physics of Neutron Star Interiors*, Ed.s D. Blaschke, N.K. Glendenning, and A.D. Sedrakain, Springer; astro-ph/0103015.
- [2] V. Petrosian, G. Beaudet, and E.E. Salpeter, *Phys. Rev.* **154** (1967) 1445.
- [3] G. Beaudet, V. Petrosian, and E.E. Salpeter, *Ap.J.* **150** (1967) 979.
- [4] D.A. Dicus, *Phys.Rev.* **D6** (1972) 941.
- [5] D.A. Dicus, E.W. Kolb, D.N. Schramm, and D.L. Tubbs, *Ap.J.* **210** (1976) 481.
- [6] N. Itoh and Y. Kohyama, *Ap.J.* **275** (1983) 858.
- [7] N. Itoh, N. Matsumoto, M. Seki, and Y. Kohyama, *Ap.J.* **279** (1984) 413.
- [8] N. Itoh, Y. Kohyama, N. Matsumoto, and M. Seki, *Ap.J.* **280** (1984) 787; erratum, **404** (1993) 418.

- [9] N. Itoh, Y. Kohyama, N. Matsumoto, and M. Seki, *Ap.J.* **285** (1984) 304; erratum, **322** (1987) 584.
- [10] H. Munakata, Y. Kohyama, and N. Itoh, *Ap.J.* **296** (1985) 197; erratum, **304** (1986) 580.
- [11] Y. Kohyama, N. Itoh, and H. Munakata, *Ap.J.* **310** (1986) 815.
- [12] H. Munakata, Y. Kohyama, and N. Itoh, *Ap.J.* **316** (1987) 708.
- [13] P.J. Schinder, D.N. Schramm, P.J. Wiita, S.H. Margolis, and D.L. Tubbs, *Ap.J.* **313** (1987) 531.
- [14] N. Itoh, T. Adachi, M. Nakagawa, Y. Kohyama, and H. Munakata, *Ap.J.* **339** (1989) 354; erratum, **360** (1990) 741.
- [15] N. Itoh, K. Kojo, and M. Nakagawa, *Ap.J. Suppl.* **74** (1990) 291.
- [16] E. Braaten, *Phys.Rev.Lett.* **66** (1991) 1655.
- [17] N. Itoh, H. Mutoh, A. Hikita, and Y. Kohyama, *Ap.J.* **395** (1992) 622; erratum, **404** (1993) 418.
- [18] Y. Kohyama, N. Itoh, A. Obama, and H. Mutoh, *Ap.J.* **415** (1993) 267.
- [19] E. Braaten and D. Segel, *Phys.Rev.* **D48** (1993) 1478.
- [20] Y. Kohyama, N. Itoh, A. Obama, and H. Hayashi, *Ap.J.* **431** (1994) 761.
- [21] M. Haft, G. Raffelt, and A. Weiss, *Ap.J.* **425** (1994) 222; erratum, **438** (1995) 1017.
- [22] N. Itoh, H. Hayashi, A. Nishikawa, and Y. Kohyama, *Ap.J.S.* **102** (1996) 411.
- [23] S. Esposito, G. Mangano, G. Miele, I. Picardi, and O. Pisanti, *Mod. Phys. Lett.* **17** (2002) 491.
- [24] M. Passera, *Phys. Rev.* **D64** (2001) 113002.
- [25] S. Esposito, G. Mangano, G. Miele, and O. Pisanti, *Phys. Rev.* **D58** (1998) 105023.

- [26] S. Esposito, G. Mangano, G. Miele, and O. Pisanti, *Nucl. Phys.* **B540** (1999) 3.
- [27] K. Ahmed and S.S. Masood, *Annals Phys.* **207** (1991) 460.
- [28] H.A. Weldon, *Phys. Rev.* **D26** (1982) 1394.